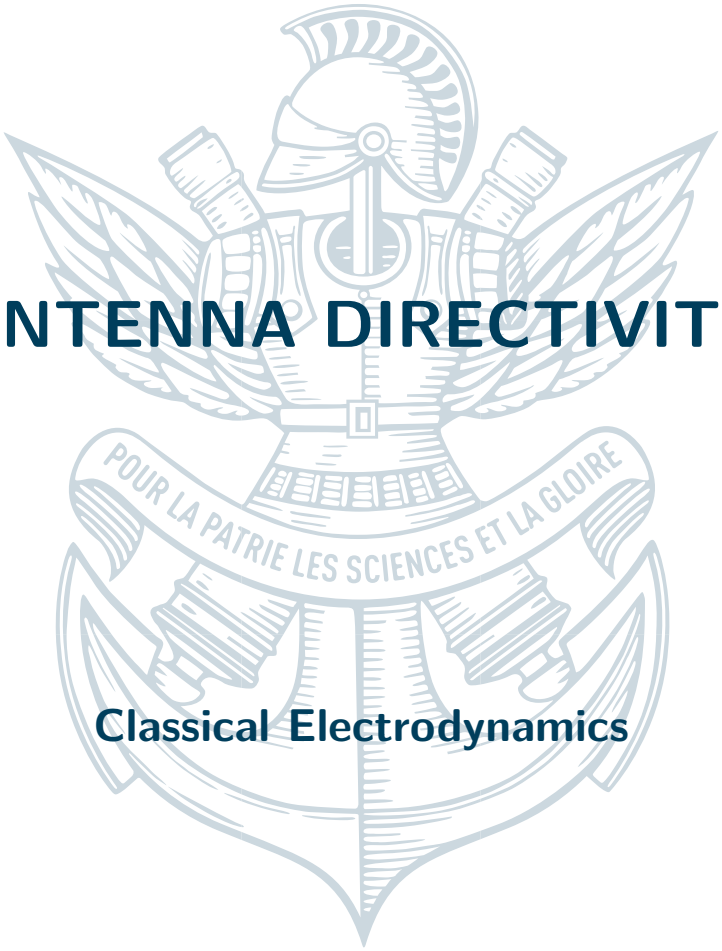

ANTENNA DIRECTIVITY

Classical Electrodynamics

2025

Yanis Tazi
Armand Fremy
Maxim Botbol
Matthéo Chauvancy

IP PARIS

CONTENTS

1 OUTLINE

The aim and thread of this report is to investigate the notion of directivity of a network of antennas. Antennas play a fundamental role in the transmission and reception of electromagnetic (denoted EM from now on report) waves. Their ability to efficiently radiate and capture energy is paramount and a key factor in determining the efficiency of antenna's is the directivity. Our project aims to bring to light this factor by simulating multiple antenna configurations. To properly investigate this subject, we have divided our project in 4 sections. We start by setting up the mathematical structure of the radiation field, essential to the simulation of directivity of antennas. Although being abstract, it is the basis of all simulations made later. We then introduce antenna parameters and discuss their role in light of the project. Multiple linear wire configurations where then explored to be able to simulate the different radiation patterns. We have chosen three setups and described the EM-field produced by standard wire antennas. The three first sections aim to build up the foundations used in the simulations and justify each element of our programs. Multiple simulations were made, looking at multiple different setups and simulating the radiation patterns and directivity of such antennas.

The results of our study of antennas are the simulations. The report aims to build up and justify the programs written. The link to the programs can be found and the appendix. Furthermore, long calculations were placed inside the appendix for the sake of clarity of the report and are at the discretion of the reader. Further justification of methods used are in the appendix.

2 RADIATING FIELDS

Please note that we will construct models that reflect ideal cases for convenience, and we will try every time to inform the reader about the implications and the limits of these models. For instance, we neglect the ground effect, that in practice might have a large impact. A more detailed introduction can be found in the Appendix.

Our first assumption is that, throughout this report, the field will be propagating in a linear, homogeneous and isotropic medium. For practical reasons, we are mostly interested in the far-field radiation, in air, that may be approximated as vacuum.

2.1 General introduction

This section aims to introduce how a given distribution of currents and charges can generate and radiate electromagnetic waves. Typically, the current distribution is localized in some region of space (in particular for currents on a wire antenna). The current source generates electromagnetic fields, which can propagate to far distances from the source location. As we shall see, it proves convenient to work with the electric and magnetic potentials rather than the electric and magnetic fields themselves.
We have seen that Maxwell's equations allow for wave solutions representing light or more generally, electromagnetic radiation. But how do you generate these waves from a collection of electric charges? In other words, how do you make light?

We know that a stationary electric charge produces a stationary electric field. If we boost this charge so it moves at a constant speed, it produces a stationary magnetic field. In this section, we will see that propagating

electromagnetic waves are created by accelerating charges.

We start by solving Maxwell's Equations in their full generality:

$$\nabla \cdot \mathbf{E} = \frac{\rho}{\epsilon_0} \qquad \nabla \cdot \mathbf{B} = 0$$

$$\nabla \times \mathbf{E} = -\frac{\partial \mathbf{B}}{\partial t} \quad \nabla \times \mathbf{B} = \mu_0 \mathbf{j} + \frac{1}{c^2}\frac{\partial \mathbf{E}}{\partial t}$$

with $c^2 = \frac{1}{\epsilon_0 \mu_0}$
The sources we will consider throughout these notes are neither static nor quasi-static, it is exactly this that will lead to radiation and retardation. In these notes we will consider the inhomogeneous wave equation and derive explicit formulae for the radiation fields as integrals over the source densities whilst using a field line analysis to show how fields that are recognizably connected to their sources "break free" and evolve into freely propagating waves.

We use the Laplacian in the scalar and vector fields to obtain the inhomogeneous wave equations of the **E** and **B** field from the Maxwell's Equations

$$\nabla^2 \mathbf{E} - \frac{1}{c^2}\frac{\partial^2 \mathbf{E}}{\partial t^2} = \frac{1}{\epsilon_0}\nabla \rho + \mu_0 \frac{\partial \mathbf{j}}{\partial t},$$

$$\nabla^2 \mathbf{B} - \frac{1}{c^2}\frac{\partial^2 \mathbf{B}}{\partial t^2} = -\mu_0 \nabla \times \mathbf{j}.$$

These two equations are not easy to manipulate, so let us consider the scalar potential V and vector potential **A**.
The vector potential **A** satisfies:

$$\mathbf{B} = \nabla \times \mathbf{A} \tag{1}$$

And the existence of a scalar potential V such that

$$\boldsymbol{E} = -\nabla V - \frac{\partial \boldsymbol{A}}{\partial t} \tag{2}$$

Up to modifying these two potentials according to *gauge transformation* (cf. Appendix), we select the *Lorenz Gauge* such that the unique potentials satisfy:

$$\nabla \cdot \mathbf{A} + \frac{1}{c^2}\frac{\partial V}{\partial t} = 0$$

Hence, Maxwell's equations reduce to the following simpler set of inhomogeneous wave equations.

$$\nabla^2 V - \frac{1}{c^2}\frac{\partial^2 V}{\partial t^2} = -\frac{\rho}{\epsilon_0}, \tag{3}$$

$$\nabla^2 \mathbf{A} - \frac{1}{c^2}\frac{\partial^2 \mathbf{A}}{\partial t^2} = -\mu_0 \mathbf{j}. \tag{4}$$

These two results are usually called retarded potentials. We summarize them below:

$$V(\boldsymbol{r}, t) = \frac{1}{4\pi\epsilon_0}\int_{\mathrm{V}} d^3 r' \frac{\rho(\boldsymbol{r}', t - |\boldsymbol{r} - \boldsymbol{r}'|/c)}{|\boldsymbol{r} - \boldsymbol{r}'|} \tag{5}$$

$$\boldsymbol{A}(\boldsymbol{r}, t) = \frac{\mu_0}{4\pi}\int_{\mathrm{V}} d^3 r' \frac{\boldsymbol{j}(\boldsymbol{r}', t - |\boldsymbol{r} - \boldsymbol{r}'|/c)}{|\boldsymbol{r} - \boldsymbol{r}'|} \tag{6}$$

where $\boldsymbol{r}'$ is a source point in V, and $\boldsymbol{r}$ the observation point.

The retardation is a consequence of the finite speed of light. Indeed, what happens at time t', at position $\boldsymbol{r}'$ will be felt at position $\boldsymbol{r}$ at a later time $t' + |\boldsymbol{r} - \boldsymbol{r}'|/c)$, that is, the change at the source point is not felt instantaneously at the observation point, but takes $|\boldsymbol{r} - \boldsymbol{r}'|/c$ (seconds) to get there as it propagates at the speed of light c.

A further detail of these calculations can be found in the appendix.

2.2 Single-frequency waves

Here, we are primarily interested harmonic time dependent waves which represents a very useful approach for studying antennas radiation pattern.

We will show that, based on this assumption, we can write $\boldsymbol{E}$ and $\boldsymbol{B}$ as a function of $\boldsymbol{A}$ only, i.e. the electromagnetic fields can be deduced only knowing the current distribution.

Every quantity has an harmonic time dependence, with wave frequency ω. We start be rewriting the potentials as

$$V(\boldsymbol{r}, t) = V(\boldsymbol{r})e^{i\omega t} \quad \boldsymbol{A}(\boldsymbol{r}, t) = \boldsymbol{A}(\boldsymbol{r})e^{i\omega t}$$

Likewise for the source densities:

$$\rho(\boldsymbol{r}, t) = \rho(\boldsymbol{r})e^{i\omega t} \quad \boldsymbol{j}(\boldsymbol{r}, t) = \boldsymbol{j}(\boldsymbol{r})e^{i\omega t}$$

In eq.(5) and (6), this yields:

$$V(\boldsymbol{r})e^{i\omega t} = \frac{1}{4\pi\epsilon_0}\int_{\mathrm{V}} d^3r' \frac{\rho(\boldsymbol{r}')e^{i\omega(t-|\boldsymbol{r}-\boldsymbol{r}'|/c)}}{|\boldsymbol{r}-\boldsymbol{r}'|} \implies V(\boldsymbol{r}) = \frac{1}{4\pi\epsilon_0}\int_{\mathrm{V}} d^3r' \frac{\rho(\boldsymbol{r}')e^{-i\omega|\boldsymbol{r}-\boldsymbol{r}'|/c}}{|\boldsymbol{r}-\boldsymbol{r}'|} \tag{7}$$

$$\boldsymbol{A}(\boldsymbol{r})e^{i\omega t} = \frac{\mu_0}{4\pi}\int_{\mathrm{V}} d^3r' \frac{\boldsymbol{j}(\boldsymbol{r})e^{i\omega(t-|\boldsymbol{r}-\boldsymbol{r}'|/c)}}{|\boldsymbol{r}-\boldsymbol{r}'|} \implies \boldsymbol{A}(\boldsymbol{r}) = \frac{\mu_0}{4\pi}\int_{\mathrm{V}} d^3r' \frac{\boldsymbol{j}(\boldsymbol{r}')e^{-i\omega|\boldsymbol{r}-\boldsymbol{r}'|/c}}{|\boldsymbol{r}-\boldsymbol{r}'|} \tag{8}$$

Now, since $\partial_t\psi = i\omega\psi$ and $\partial_t^2\psi = -\omega^2\psi$ for $\psi = V, \boldsymbol{A}$, we can rewrite the two wave equations (3) and (4) as follows:

$$\nabla^2 V + k^2 V = -\frac{\rho}{\epsilon_0}$$
$$\nabla^2 \boldsymbol{A} + k^2 \boldsymbol{A} = -\mu_0 \boldsymbol{j}$$

as well as the Lorenz gauge:

$$\nabla \cdot \boldsymbol{A} + i\frac{\omega}{c^2}V = \nabla \cdot \boldsymbol{A} + i\omega\mu_0\epsilon_0 V = 0$$

where we have used the dispersion relation $k = \omega/c$.

In the end, we get:

$$\boldsymbol{E} = -\nabla V - \frac{\partial \boldsymbol{A}}{\partial t} = \frac{1}{i\omega\mu_0\epsilon_0}\nabla(\nabla \cdot \boldsymbol{A}) - i\omega\boldsymbol{A} = \frac{1}{i\omega\mu_0\epsilon_0}\left[\nabla(\nabla \cdot \boldsymbol{A}) + k^2\boldsymbol{A}\right]$$

since $c^2 = \frac{1}{\epsilon_0\mu_0}$.

Using the identity $\nabla \times (\nabla \times \mathbf{A}) = \nabla(\nabla \cdot \mathbf{A}) - \nabla^2\mathbf{A}$ we can rewrite the E-field in a more convenient form:

$$\boldsymbol{E} = \frac{1}{i\omega\mu_0\epsilon_0}\left[\nabla \times (\nabla \times \mathbf{A}) + \nabla^2\mathbf{A} + k^2\boldsymbol{A}\right] = \frac{1}{i\omega\mu_0\epsilon_0}\left[\nabla \times (\nabla \times \mathbf{A}) - \mu_0\boldsymbol{j}\right] \tag{9}$$

The last term can be removed in regions where there is no current ($\boldsymbol{j} = \mathbf{0}$), which will always be the case when studying the radiation pattern generated away from the antenna.

The B-field remains the same:

$$\boldsymbol{B} = \nabla \times \boldsymbol{A} = \mu_0 \boldsymbol{H} \tag{10}$$

with $\boldsymbol{A}(\boldsymbol{r}) = \frac{\mu_0}{4\pi} \int_V d^3r' \frac{\boldsymbol{j}(\boldsymbol{r}')e^{-i\omega|\boldsymbol{r}-\boldsymbol{r}'|/c}}{|\boldsymbol{r}-\boldsymbol{r}'|}$ and ω the angular frequency of the wave.

2.3 Far field radiations

Equations (7) and (8) relates the potentials to their sources $\rho(\boldsymbol{r}')$ and $\boldsymbol{j}(\boldsymbol{r}')$ with a time retardation:

$$V(\boldsymbol{r}) = \frac{1}{4\pi\varepsilon_0} \int_V \frac{\rho(\boldsymbol{r}')\, e^{-ik|\boldsymbol{r}-\boldsymbol{r}'|}}{|\boldsymbol{r}-\boldsymbol{r}'|}\, \mathrm{d}^3r', \tag{11}$$

$$\boldsymbol{A}(\boldsymbol{r}) = \frac{\mu_0}{4\pi} \int_V \frac{\boldsymbol{j}(\boldsymbol{r}')\, e^{-ik|\boldsymbol{r}-\boldsymbol{r}'|}}{|\boldsymbol{r}-\boldsymbol{r}'|}\, \mathrm{d}^3r'. \tag{12}$$

where $k = \omega/c$. Recall that we integrate over V which is the volume of the charge distribution.

The integrals are exact and valid at any *observation point* $\boldsymbol{r}$. We now specialize them to the *far–zone* ($r \gg r'$), retaining only the terms that contribute to outward-propagating radiation.

For an observation point $\boldsymbol{r}$ in the far zone ($r \gg r'$) we expand the separation

$$|\boldsymbol{r}-\boldsymbol{r}'| \;=\; \sqrt{r^2 - 2\boldsymbol{r}\cdot\boldsymbol{r}' + r'^2},$$

We can factor out r and use a second-order binomial (Taylor) expansion, denoting $\hat{r}$ the radial unit vector:

$$\begin{aligned} |\boldsymbol{r}-\boldsymbol{r}'| &= r\sqrt{1 - 2\frac{\mathbf{r}'\cdot\hat{\mathbf{r}}}{r} + \left(\frac{r'}{r}\right)^2} \\ &= r\left(1 + \frac{1}{2}(-2\frac{\mathbf{r}'\cdot\hat{\mathbf{r}}}{r} + \left(\frac{r'}{r}\right)^2) + \frac{1}{8}(2\frac{\mathbf{r}'\cdot\hat{\mathbf{r}}}{r})^2\right) \qquad (13) \\ &= r - \mathbf{r}'\cdot\hat{\mathbf{r}} + \frac{r'^2 + (\mathbf{r}'\cdot\hat{\mathbf{r}})^2}{2r} \qquad (14) \end{aligned}$$

Eq. (14) is the form employed in the radiation (far-field) approximation but can be further simplified as we shall see below.

To justify dropping the second-order piece $\gamma = \frac{r'^2+(\mathbf{r}'\cdot\hat{\mathbf{r}})^2}{2r}$ from both the phase and the denominator, we need two inequalities:

(i) $r \gg r'$, ensuring the source is small compared with the observation distance;

(ii) $kr'^2/r \ll \pi$, so that the phase error $k\gamma$ remains negligible (because $e^{ik\gamma}$ is 2π-periodic.)

Starting with the general retarded potential (11) and substituting the distance expansion to the first order from Eq. (14), we obtain

$$V(\mathbf{r}) = \frac{1}{4\pi\varepsilon_0} \int_V \frac{\rho(\mathbf{r}')\, e^{-ik|\mathbf{r}-\mathbf{r}'|}}{|\mathbf{r}-\mathbf{r}'|}\, \mathrm{d}^3r' \;\simeq\; \frac{1}{4\pi\varepsilon_0} \int_V \frac{\rho(\mathbf{r}')\, e^{-ik\left(r-\hat{\mathbf{r}}\cdot\mathbf{r}'\right)}}{r-\hat{\mathbf{r}}\cdot\mathbf{r}'}\, \mathrm{d}^3r', \tag{15}$$

where $\hat{\mathbf{r}} = \mathbf{r}/r$ and $k = 2\pi/\lambda$.

As seen in *Wave Optics*, in the Fraunhofer radiation zone we may simplify the denominator a little further by replacing $|\boldsymbol{r} - \boldsymbol{r}'| \approx r$ while leaving the $\hat{\mathbf{r}}\cdot\mathbf{r}'$ term inside the phase (we approximate via parabolic waves). This gives:

$$V_{\text{far}}(\mathbf{r}) = \frac{e^{-ikr}}{4\pi\varepsilon_0\, r}\int_V \rho(\mathbf{r}')\, e^{ik\hat{\mathbf{r}}\cdot\mathbf{r}'}\,\mathrm{d}^3r'. \tag{16}$$

Although this "mixed" approximation (different treatment of $|\boldsymbol{r} - \boldsymbol{r}'|$ in the phase and the denominator) might look inconsistent at first glance, it is usually acceptable for radiation problems: the neglected terms only affect evanescent or reactive fields, not the outward-propagating $1/r$ wave that concerns us here.

If we replace the typical source dimension by l (roughly the largest separation inside the antenna), inequalities (i) and (ii) become:

$$r \gg l \quad \text{and} \quad r \gg \frac{2l^2}{\lambda}.$$

For most practical antennas (e.g half-wave antenna) $l \sim \lambda$, so the second condition is essentially covered by the first. Together they define what we have called the *Fraunhofer* or *far-field* region. Similarly, for the vector potential we arrive at the familiar far-field forms for both *scalar* and *vector* potentials:

$$V(\mathbf{r}) = \frac{e^{-ikr}}{4\pi\varepsilon_0\, r}\int_V \rho(\mathbf{r}')\, e^{\,i\mathbf{k}\cdot\mathbf{r}'}\,\mathrm{d}^3r', \tag{17}$$

$$\mathbf{A}(\mathbf{r}) = \frac{\mu_0\, e^{-ikr}}{4\pi\, r}\int_V \mathbf{j}(\mathbf{r}')\, e^{\,i\mathbf{k}\cdot\mathbf{r}'}\,\mathrm{d}^3r', \qquad \mathbf{k} = k\,\hat{\mathbf{r}}. \tag{18}$$

Here all explicit radial dependence, e^{-ikr}/r, has been separated out; the remaining integral factors carry the directional (θ, φ) behaviour. For convenience we denote these angular factors by

$$\boxed{Q(\theta,\varphi) = \int_V \rho(\mathbf{r}')\, e^{\,i\mathbf{k}\cdot\mathbf{r}'}\,\mathrm{d}^3r', \qquad \mathbf{F}(\theta,\varphi) = \int_V \mathbf{j}(\mathbf{r}')\, e^{\,i\mathbf{k}\cdot\mathbf{r}'}\,\mathrm{d}^3r'}.$$

Now we aim to show that, in the far field, the gradient operator ∇ can be approximated by $-\,i\,k$, exactly as one does for plane waves. We begin by recalling the curl operator in spherical coordinates:

$$\nabla\times\mathbf{X} = \hat{\mathbf{r}}\,\frac{1}{r\sin\theta}\big[\partial_\theta(\sin\theta\, X_\varphi) - \partial_\varphi X_\theta\big] + \hat{\boldsymbol{\theta}}\,\frac{1}{r}\big[\tfrac{1}{\sin\theta}\partial_\varphi X_r - \partial_r(rX_\varphi)\big] + \hat{\boldsymbol{\varphi}}\,\frac{1}{r}\big[\partial_r(rX_\theta) - \partial_\theta X_r\big].$$

We are going to apply this curl to the radiation vector potential

$$\mathbf{A}(\mathbf{r}) = \frac{\mu_0\, e^{-ikr}}{4\pi r}\,\mathbf{F}(\theta,\varphi) \propto \frac{1}{r},$$

Notice, substituting $\mathbf{A}$, we can factor out of all partial derivatives with respect to φ and θ the $1/r$ term:

$$\frac{1}{r\sin\theta}\big[\partial_\theta(\sin\theta\, A_\varphi) - \partial_\varphi A_\theta\big] \propto \frac{1}{r^2}, \quad \frac{1}{r}\big[\tfrac{1}{\sin\theta}\partial_\varphi A_r\big] \propto \frac{1}{r^2}, \quad \frac{1}{r}\big[-\partial_\theta A_r\big] \propto \frac{1}{r^2}$$

$$\nabla\times\mathbf{A} = \big(\hat{\mathbf{r}}\,\partial_r + O(1/r)\big)\times\frac{\mu_0\, e^{-ikr}}{4\pi r}\,\mathbf{F} \;\simeq\; -ik\,(\hat{\mathbf{r}}\times\mathbf{F})\frac{\mu_0\, e^{-ikr}}{4\pi r} = -\,i\,\mathbf{k}\times\mathbf{A} \quad (\mathbf{k} = k\hat{\mathbf{r}}),$$

assuming that we can neglect all terms $\mathcal{O}(1/r^2)$, with respect to $\frac{1}{r}$ dependent terms, for $r \gg 1$ in the far-field.

Thus, for any function of the form $f(\theta,\varphi)\, e^{-ikr}/r$ we may, to leading order in $1/r$, replace the gradient operator by

$$\nabla \;\longrightarrow\; -i\,\mathbf{k} = -ik\,\hat{\mathbf{r}} \qquad (r \to \infty).$$

We now have all the tools to compute the radiation fields where we can simplify their expression at far distances.

In fact, in order to compute the E and H radiation fields, we can now use the E-field equation (Eq.9 in the report), for $\boldsymbol{j} = \mathbf{0}$ (no current) far from the source:

$$\begin{aligned}\mathbf{E} &= \frac{1}{i\omega\mu_0\varepsilon_0}\Big[\nabla\times(\nabla\times\mathbf{A}) \;-\; \mu_0\mathbf{j}\Big] \\ &= \frac{ik\,\eta}{4\pi r}\, e^{-ikr}\,\hat{\mathbf{r}}\times\big(\hat{\mathbf{r}}\times\mathbf{F}\big),\end{aligned}$$

with $\eta = \sqrt{\epsilon_0/\mu_0}$ (defined in the Appendix).

Since $\omega = ck$ and $c = 1/\sqrt{\mu_0\varepsilon_0}$, it follows that

$$\omega\mu_0 \;=\; k\sqrt{\frac{\mu_0}{\varepsilon_0}} \;=\; k\eta.$$

For $\mathbf{H}$ we proceed in the same way, observing

$$\mathbf{H} = \frac{1}{\mu_0}\boldsymbol{B} \;=\; \frac{1}{\mu_0}\nabla\times\mathbf{A} \;\simeq\; -\frac{i}{\mu_0}\,\mathbf{k}\times\mathbf{A} \;=\; -\frac{ik}{4\pi r}\, e^{-ikr}\,\hat{\mathbf{r}}\times\mathbf{F}.$$

Therefore, writing

$$\mathbf{F} = F_r\,\hat{\mathbf{r}} + F_\theta\,\hat{\boldsymbol{\theta}} + F_\varphi\,\hat{\boldsymbol{\varphi}}, \qquad \mathbf{F}_\perp = F_\theta\,\hat{\boldsymbol{\theta}} + F_\varphi\,\hat{\boldsymbol{\varphi}},$$

Since $\hat{\mathbf{r}}\times\hat{\mathbf{r}} = \mathbf{0}$, $\hat{\mathbf{r}}\times\hat{\boldsymbol{\theta}} = -\hat{\boldsymbol{\varphi}}$ and $\hat{\mathbf{r}}\times\hat{\boldsymbol{\varphi}} = \hat{\boldsymbol{\theta}}$, our final far-fields are

$$\boxed{\mathbf{E} = -\frac{ik\,\eta}{4\pi r}\, e^{-ikr}\,\mathbf{F}_\perp, \qquad \mathbf{H} = -\frac{ik}{4\pi r}\, e^{-ikr}\,\hat{\mathbf{r}}\times\mathbf{F}_\perp} \quad \text{(radiation fields)}.$$

3
ANTENNA'S PARAMETERS

Inspired from [1], this chapter is summarizing the relevant characteristics of an antenna, in order to perform analysis later on.

3.1 Reminders on Energy Propagation

The quantity used to describe the power associated with an electromagnetic wave is the instantaneous *Poynting vector* defined as

$$\boldsymbol{\Pi} = \boldsymbol{E} \times \boldsymbol{H} = \frac{1}{\mu_0} \boldsymbol{E} \times \boldsymbol{B} \text{ in } [W \cdot m^{-2}]$$

It is pointing along the direction of the wave propagation. It has the dimension of a power per surface, so it is a radiation density.

For applications of time-varying fields, it is often more desirable to find the average power density which is obtained by integrating the instantaneous Poynting vector over one period and dividing by the period. Since we are mainly dealing with time-harmonic varying fields, the average Poynting vector is simply

$$\langle \boldsymbol{\Pi} \rangle_t = \frac{1}{2} \operatorname{Re} \{ \mathbf{E} \times \mathbf{H}^* \}$$

Radiation intensity in a given direction is defined as "the power radiated from an antenna per unit solid angle." The radiation intensity is a far-field parameter, and it can be obtained by simply multiplying the radiation density by the square of the distance. In mathematical form it is expressed as

$$U = r^2 | \langle \boldsymbol{\Pi} \rangle_t | \text{ in } [W]$$

It is also common to measure this quantity in decibels, which is a simple conversion of the above expression:

$$U_{dB} = 10 \times log_{10}(U) \text{ in } [dB]$$

From this, we deduce also the *average power* radiated by an antenna, by integrating over a closed surface surrounding the charged region:

$$P_{rad} = \iint_S \langle \boldsymbol{\Pi} \rangle_t \, d\boldsymbol{S} = \iint_\Omega U d\Omega$$

with $d\boldsymbol{S}$ oriented normally to the surface and the solid angle $d\Omega = \sin\theta d\theta d\phi$ in spherical coordinates. We notice that, in the special case of isotropic source, U is invariant with ϕ and θ with the spherical symmetry, and so $P_{rad-iso} = 4\pi U$

3.2 Directivity

We have yet to define a measure of *directivity*, to this end we associate to an antenna pattern its *beamwidth*. The beamwidth of a pattern is defined as the angular separation between two identical points on opposite side of the pattern maximum. In an antenna pattern, there are a number of beamwidths. One of the most widely used beamwidths is the Half-Power Beamwidth (HPBW or 3dB-beamwidth), which is defined by IEEE [1] as: "In a plane containing the direction of the maximum of a beam, the angle between the two directions in which the radiation intensity is one-half value of the beam." i.e. as the angular width (in degrees) of the main lobe of the antenna's radiation pattern between the points where the power drops to half its maximum value. It indicates the angle over which most of the antenna's energy is concentrated. A narrow beamwidth means the antenna is more focused (like a spotlight), while a wide beamwidth means it's more spread out (like a floodlight).

This must not be mistaken with *bandwidth* of an antenna, which is defined as "the range of frequencies within which the performance of the antenna, with respect to some characteristic, conforms to a specified standard." The bandwidth can be considered to be the range of frequencies, on either side of a center frequency (usually the resonance frequency for a dipole), where the antenna characteristics (pattern, gain, beam direction, radiation

[1] Institute of Electrical and Electronics Engineers

efficiency) are within an acceptable value of those at the center frequency.

It is now time to define the main concept of this report: *directivity*. Indeed, in practice, antennas (or array of antennas as we shall see) must also serve as a directional devise (i.e. accentuate the radiation energy in some directions and suppress it in others) in addition to a probing devise. The directivity of an antenna is a dimensionless quantity defined as "the ratio of the radiation intensity in a given direction from the antenna to the radiation intensity averaged over all directions". In other words, the directivity of a non-isotropic source is equal to the ratio of its radiation intensity in a given direction over that of an isotropic source.

$$D = \frac{U}{U_0} = \frac{4\pi U}{P_{rad}}$$

where $U_0 = \frac{1}{4\pi}\int_0^{\pi}\int_0^{2\pi} I(r,\theta,\phi)r^2 \sin\theta d\theta d\phi$ is the average intensity radiated by the antenna in all directions. And so the maximum directivity is evidently equal to $D_{max} = \frac{U_{max}}{U_0}$, with U_{max} the maximum intensity radiated in a specific direction. As we could have expected, this quantity does not depend on the distance r from the origin, which makes sense since the directivity should be related to an orientation, not how far you are from the source.

Another useful concept is *gain*, which is what one really cares about in practice when designing a real antenna. Gain of an antenna (in a given direction) is defined as "the ratio of the intensity U, in a given direction, to the radiation intensity that would be obtained if the power accepted by the antenna were radiated isotopically". It must not be confused with directivity as it is a measure that takes into account the efficiency of the antenna as well as its directional capabilities. The radiation intensity corresponding to the isotopically radiated power is equal to the power accepted (input) by the antenna divided by 4π (because $U_{isotropic} = U_{in}$ independent of θ and ϕ). This can be expressed as:

$$Gain = \frac{4\pi U}{P_{in}}$$

As an analogy to avoid confusion: we can think of directivity as how focused your flashlight beam is in a given direction, and efficiency as how bright the bulb actually is compared to input power (some energy might just heat the bulb, not produce light). Gain is how bright the flashlight appears in the direction it's pointed. For instance, for an isotropic dipole, directivity is $D = 1$, while we could have $Gain < 1$ (considering some losses - e.g heat - in the process of radiation).

In our setup, we are not concerned about losses occurring within the system, but about the directional capacities of the antenna so we may use directivity as a sufficient analysis tool.

Taking the log of the directivity lets us easily interpret how much more power the antenna radiates in a given direction compared to an isotropic radiator because, for an isotropic emitting source, $log_{10}(D) = log_{10}(1) = 0$ meaning that an arbitrary source with $log_{10}(D) > 0$ is more directive in this direction that an isotropic source (and conversely for $log_{10}(D) < 0$).

4
LINEAR WIRE ANTENNA

The purpose of this section is to derive our first set of equations describing the EM-field produced by standard wire antennas.
There are three different regions to consider: far-field or Fraunhofer ($kr \gg 1$), near-field or Fresnel ($kr \ll 1$)

and intermediate region ($kr > 1$).

We are assuming first an antenna of finite length, emitting at a single frequency ω, with negligible thickness. We choose our z-axis to be aligned with the antenna orientation. No assumption is made on the current yet.

To reduce the mathematical complexities, it will be assumed in this chapter that the dipole has a negligible diameter (ideally zero). This is a good approximation provided the diameter is considerably smaller than the operating wavelength and that we are looking for the far-field.

A schematic view of the system would be:

$$\text{current source} \rightarrow \text{transmission lines} \rightarrow \text{antenna} \rightarrow \text{free space radiation}$$

The guiding devise or transmission line is a waveguide used to transport EM energy from the source to the antenna (transmitting antenna), or from the antenna to the receiver (receiving antenna in which case the arrows are reversed). The source is creating an alternating current in order to accelerate electrons: $\frac{dI_z}{dt} = \rho_l a_z$, with ρ_l the charge per unit length (Note that for loop antenna, a DC current is sufficient to generate radiation, since charges rotating at constant speed along a loop are subject to an acceleration). For the two-wire balanced (symmetrical) transmission line, the current in a half cycle of one wire is of the same magnitude but 180° out-of-phase from that in the corresponding half-cycle of the other wire. If in addition the spacing between the two wires is very small, the fields radiated by the current of each wire are essentially cancelled by those of the other. The net result is an almost ideal (and desired) non-radiating transmission line. We will thus place ourselves in this ideal case where there is a no net radiation by the (lossless) transmission line system because the fields radiated by one cancel those of the other due to a π-phase difference (even if it is not necessarily and exactly the case in practice).

For the sake of completeness we first consider the simple case of thin dipole antenna with a harmonic current.

4.1 Thin wire antenna

For a *thin wire* antenna, we can already write the current density as follows:

$$\boldsymbol{j}(x, y, z, t) = I(z)\delta(x)\delta(y)e^{i\omega t}\boldsymbol{e}_z$$

Keeping the spatial term:

$$\boldsymbol{j}(x, y, z) = I(z)\delta(x)\delta(y)\boldsymbol{e}_z \tag{19}$$

Inserting in Eq.8, and integrating with respect to x' and y', the vector potential reads:

$$\boldsymbol{A}(\boldsymbol{r}) = \frac{\mu_0}{4\pi}\boldsymbol{e}_z \int_\Gamma dz' \frac{I(z')e^{-i\omega R/c}}{R}, \quad R = |\boldsymbol{r} - \boldsymbol{r}'| = \sqrt{\boldsymbol{\rho}^2 + (z - z')^2} \tag{20}$$

with Γ the length of the antenna. So we see that $\boldsymbol{A}$ has only a z-component.

According to Eq.9 and Eq.10, we can write the components of the electric and magnetic field as:

$$E_z = \frac{1}{i\omega\mu_0\epsilon_0}(\partial_z^2 A_z + k^2 A_z) \tag{21}$$

$$E_\rho = \frac{1}{i\omega\mu_0\epsilon_0}(\partial_\rho \partial_z A_z) \tag{22}$$

$$B_\phi = -\partial_\rho A_z \tag{23}$$

This general result is crucial and will be useful also for the chapter on antenna arrays.

Since we want our emitted signal to travel far away, allowing long-distance communication, we will begin to focus on Fraunhofer region to simplify the above equations. In a second time, we will derive the near-field interaction within a set of closely spaced antennas (see Arrays section).

4.2 Dipole antenna

The simplest linear antenna configuration is the dipole that has a current distribution $I(z) = I_0 l\delta(z)$ and so a current density of $\boldsymbol{j}(x, y, z) = I_0 l\delta(z)\delta(x)\delta(y)\boldsymbol{e}_z$ corresponding to an infinitesimally small (and thin) antenna located at the origin. First we compute $\boldsymbol{F}$. It will have only a z-component given by:

$$F_z(\theta) = \int_{-l/2}^{l/2} I(z')e^{jkz'\cos\theta}dz' = \int_{-l/2}^{l/2} I_0\delta(z')e^{jkz'\cos\theta}dz' = lI_0$$

Thus, $\boldsymbol{F}_\perp = \hat{\boldsymbol{\theta}}F_z \sin\theta$. The radiation fields are:

$$\mathbf{E} = -\frac{jk\,\eta}{4\pi r}\, e^{-jkr}e^{j\omega t}\, F_z \sin\theta\hat{\boldsymbol{\theta}}, \qquad \mathbf{H} = -\frac{jk}{4\pi r}\, e^{-jkr}e^{j\omega t}\, F_z \sin\theta\hat{\boldsymbol{\phi}}$$

The average Poynting vector and the radiation intensity are then given by:

$$\langle\boldsymbol{\Pi}\rangle_t = \frac{k^2\,\eta}{32\pi^2 r^2} l^2|I_0|^2 \sin^2\theta\hat{\boldsymbol{r}}, \qquad \boxed{U(\theta) = \frac{\eta k^2}{32\pi^2} l^2|I_0|^2 \sin^2\theta}$$

The 3D radiation pattern described by this equation is well-known as a torus (or donut) shape centered on the origin, invariant with ϕ with highest intensity for an angle $\theta = \pi/2$.

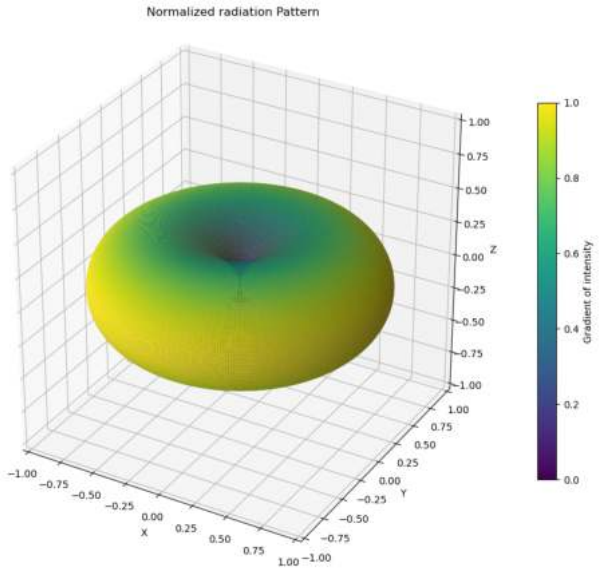

Figure 1: 3D plot radiation pattern produced by a simple dipole. You will notice that it has less directivity in θ than for a standing wave antenna (see Figure 6)

4.3 Standing wave Antenna

The configuration depicted in Figure 3 corresponds to a center-fed dipole antenna. The antenna is excited at its midpoint ($z = 0$) by a time-varying current source, which drives equal and opposite currents into each half of

the dipole. These arms extend along the z-axis from $-l/2$ to $l/2$, forming a symmetric structure. The current propagates outward from the feed point along the conductive elements, and due to the open-circuit condition at the physical ends of the antenna, the current amplitude necessarily drops to zero at those extremities.

When the current arrives at the end of each of the wires, it undergoes a complete reflection (equal magnitude and 180° phase reversal). The reflected traveling wave, when combined with the incident traveling wave, forms in each wire a pure standing wave pattern of sinusoidal form (see expression below).

Looking at Figure 3, the upper part and the lower part are not directly connected. They are connected through the feeding source (the generator and transmission lines), which pushes current into the top arm and pulls current from the bottom arm. Current must flow from one terminal of the generator to the other. When the voltage from the generator is positive at the top relative to the bottom, current flows into the upper half and out of the lower half. Half a period later, when the generator voltage reverses sign, the currents also reverse direction, now into the bottom and out of the top. This oscillates sinusoidally at the (angular) frequency ω.

Consequently, the charges (electrons) in the metal oscillate back and forth along the antenna creating EM-waves.

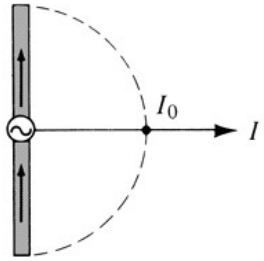

Figure 2: Approximated diagram of the antenna, neglecting the transmission lines

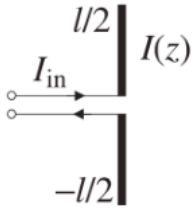

Figure 3: Diagram Standing wave antenna including transmission lines

For a very thin dipole (ideally zero diameter) centered at the origin, the current distribution can be written, to a good approximation, as:

$$I(x, y, z) = I_0 \sin\left(k(\frac{l}{2} - |z|)\right) e^{i\omega t}$$

Indeed, since no current is flowing outwards at the endpoints, $I(z = l/2) = I(z = -l/2) = 0$.
So (we omit the time-dependent factor for now, as it won't affect our calculation):

$$\vec{j}(x, y, z) = I_0 \sin\left(k(\frac{l}{2} - |z|)\right) \delta(x)\delta(y)\vec{e}_z$$

for $z \in [-\frac{l}{2}, \frac{l}{2}]$, l being the length of the antenna. This current corresponds actually to what is called a standing wave antenna. According to our researches, it has been verified experimentally that the current in a center-fed wire antenna has sinusoidal form with nulls at the end points, as shown above.

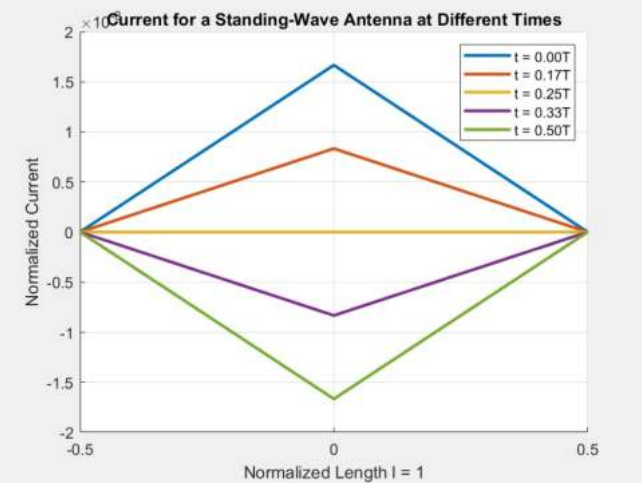

Figure 4: Current plotted at different times t (with T the oscillation period). A negative current means a change a direction. $l << \lambda$

In the far-field approximation, we have proven that, in spherical coordinates:

$$\vec{E} = -ik\eta \frac{e^{-ikr}}{4\pi r}(F_\theta \vec{e}_\theta + F_\phi \vec{e}_\phi), \qquad \vec{H} = -ik\frac{e^{-ikr}}{4\pi r}(F_\theta \vec{e}_\phi - F_\phi \vec{e}_\theta)$$

where $\eta = \sqrt{\frac{\mu}{\epsilon}}$ and $\vec{F}(\theta,\phi) = \int_V \vec{j}(r')e^{i\vec{k}\cdot\vec{r}'}d^3r'$.
Notice that, inserting the expression for $\vec{J}$, and using the properties of the delta-Dirac distribution:

$$\vec{F} = \vec{e}_z \int_{-l/2}^{l/2} I_0 \sin\left(k(\frac{l}{2} - |z'|)\right) e^{ik\cdot z'\cos(\theta)}dz'$$

where we have used $\vec{e}_z = \cos(\theta)\vec{e}_r + \sin(\theta)\vec{e}_\theta$. Also, we recall that $\vec{k}$ is pointing outwards radially.
This means that:

$$F_\theta = \sin\theta \int_{-l/2}^{l/2} I_0 \sin\left(k(\frac{l}{2} - |z|)\right) e^{ik\cdot z'\cos(\theta)}dz', \qquad F_\phi = 0$$

The proof of the following equality will be found in the appendix:

$$\int e^{ax}\sin(bx+c)dx = \frac{e^{ax}}{a^2+b^2}[a\sin(bx+c) - b\cos(bx+c)] \tag{24}$$

Integrating F_θ thanks to Eq.24:

$$\begin{aligned} F_\theta &= I_0 \sin\theta \ \frac{1}{k\sin^2\theta}\left[e^{ik\cos\theta l/2} + e^{-ik\cos\theta l/2} - 2\cos\left(\frac{kl}{2}\right)\right] \\ &= 2I_0 \frac{1}{k\sin\theta}\left[\cos(k\cos\theta l/2) - \cos\left(\frac{kl}{2}\right)\right] \end{aligned}$$

Finally, the far-fields of a standing wave antenna are given by:

$$\vec{E} = -i\eta\frac{e^{-ikr}}{2\pi r}\frac{I_0}{\sin\theta}\left[\cos\left(\cos\theta\frac{kl}{2}\right) - \cos\left(\frac{kl}{2}\right)\right]e^{i\omega t}\vec{e}_\theta$$

$$\vec{H} = -i\frac{e^{-ikr}}{2\pi r}\frac{I_0}{\sin\theta}\left[\cos\left(\cos\theta\frac{kl}{2}\right) - \cos\left(\frac{kl}{2}\right)\right]e^{i\omega t}\vec{e}_\phi$$

The verification that the dispersion relation $kc = \omega$ is valid in the far field can be found in the appendix.

The average Pointing vector can be written as:

$$\langle \mathbf{\Pi} \rangle = \frac{1}{2} \operatorname{Re} \{ \mathbf{E} \times \mathbf{H}^* \} = \frac{\eta}{8\pi^2 r^2} \frac{|I_0|^2}{\sin^2 \theta} \left[\cos\left(\cos\theta \frac{kl}{2} \right) - \cos\left(\frac{kl}{2} \right) \right]^2 \mathbf{e}_r$$

Thus,

$$\boxed{U(\theta) = \frac{\eta}{8\pi^2} \frac{|I_0|^2}{\sin^2 \theta} \left[\cos\left(\cos\theta \frac{kl}{2} \right) - \cos\left(\frac{kl}{2} \right) \right]^2}$$

Remark that the energy is indeed propagating in the radial direction. Let us observe how it varies with the length l and with the angle θ with respect to the antenna axis.

For this, we can have a look at a quantitative representation of the directivity of the antenna with the beamwidth:

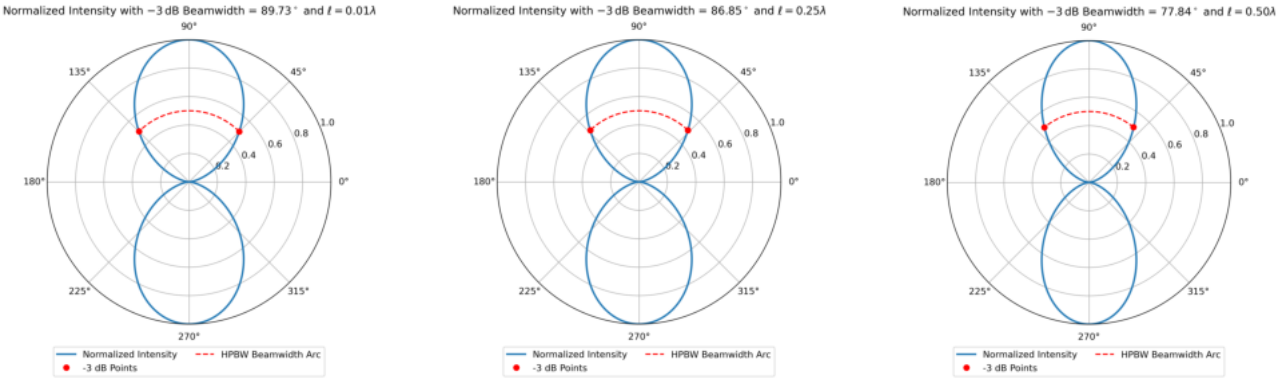

(a) $l = \lambda/100, l << \lambda$ (b) $l = \lambda/4$ (c) $l = \lambda/2$

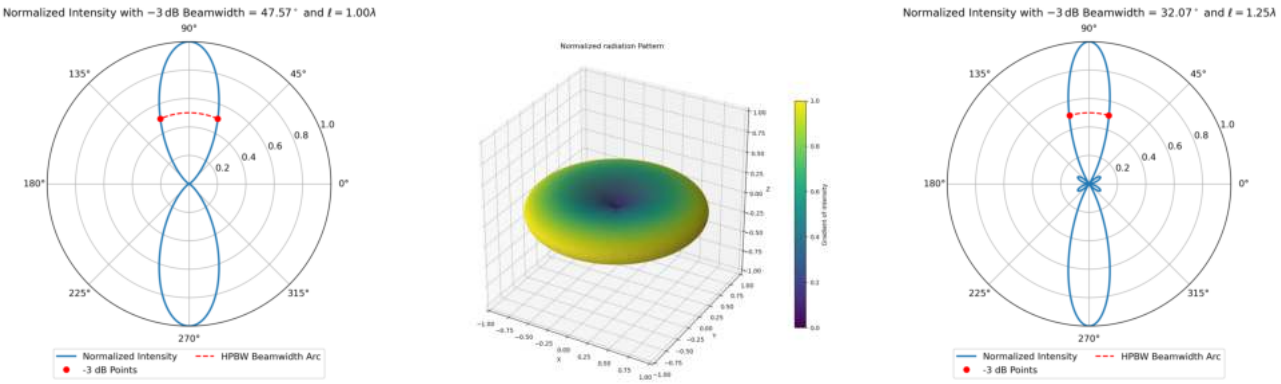

(a) $l = \lambda$ (b) 3D plot for $l = \lambda$ (c) $l = 1.25 \cdot \lambda$

Figure 6: Polar plot showing the (normalized) radiated intensity $U(\theta)/U_{max}$ versus θ, λ normalized to 1, for a standing wave antenna

The Python codes used the formula of $U(\theta, \phi)$ computed above and can be found here.

Observations:

- The maximum directivity will be found at $\theta = \pi/2$, that is perpendicular to the antenna axis.
- As the length l increases, the directivity is increased.
- Side lobes begin to appear when the length exceeds one wavelength $l > \lambda$.

One of our goal is to minimize side lobes as they represent a source of power loss.

The radiated power over all directions is given by:

$$P_{rad} = \int_0^{\pi}\int_0^{2\pi} \mathbf{\Pi}\cdot\mathbf{n}r^2\sin\theta d\theta d\phi = \int_0^{\pi}\int_0^{2\pi} \frac{\eta}{8\pi^2}\frac{|I_0|^2}{\sin\theta}\left[\cos\left(\cos\theta\frac{kl}{2}\right)-\cos\left(\frac{kl}{2}\right)\right]^2 d\theta d\phi$$
$$= \frac{\eta|I_0|^2}{4\pi}\int_0^{\pi}\frac{1}{\sin\theta}\left[\cos\left(\cos\theta\frac{kl}{2}\right)-\cos\left(\frac{kl}{2}\right)\right]^2 d\theta$$

Clearly, if $\theta = 0, \pi$, the power is zero. This reflects a more general fact, which is that no radiation is generated in the direction of acceleration of the charges.

The directivity as a function of the orientation θ (with respect to the antenna-axis) would then be:

$$D(\theta) = \frac{4\pi U(\theta)}{P_{rad}} = 2\left[\frac{\cos\left(\cos\theta\frac{kl}{2}\right)-\cos\left(\frac{kl}{2}\right)}{\sin\theta}\right]^2 \cdot \frac{1}{\int_0^{\pi}\frac{1}{\sin\theta}\left[\cos\left(\cos\theta\frac{kl}{2}\right)-\cos\left(\frac{kl}{2}\right)\right]^2 d\theta}$$

with $U(\theta) = r^2|\mathbf{\Pi}|$ the radiation intensity.

We are not able to solve by hand the integral to obtain the radiated power. Nevertheless, looking at the intensity profile, which looks like the integrand plotted as a function of the angle, we see that it is not highly peaked, but rather smooth. We can therefore solve it numerically using a discretization method that we describe in the Appendix. For a half-wave antenna, the approximated result reads:

$$P_{rad} \approx 37W$$

Then we plot the directivity as a function of θ.

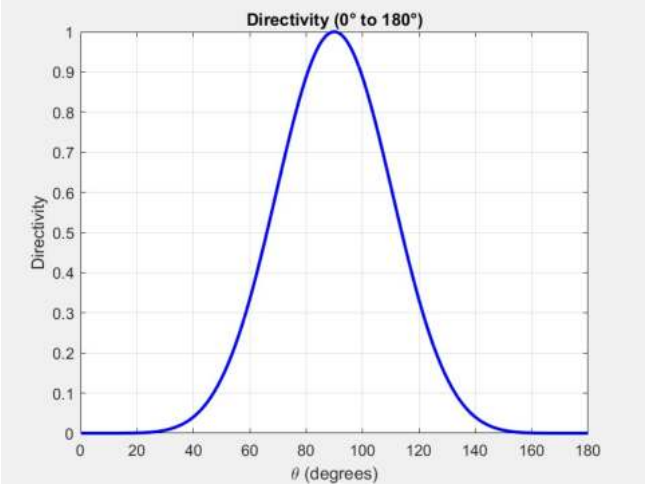

Figure 7: Directivity as a function of θ, the angle between the antenna axis $\hat{\boldsymbol{z}}$ and the observation direction $\boldsymbol{r}$. Parameters involved: $\omega = 10^8 s^{-1}$, $l = \lambda/2 = \pi/k$, $I_0 = 1$ A.

There exists some common standing wave antennas with specific characteristics that simplify this result. In addition, since for a single wire antenna the pattern is symmetric by rotation around the z-axis, the directivity is uniform with ϕ, it simply changes with the angle θ as shown above (that is if we are positioned at the antenna location, and if we look up or down).

4.4 Half-wave antenna

The half-wave dipole corresponding to $l = \lambda/2$, or $kl = \frac{2\pi}{\lambda}\frac{\lambda}{2} = \pi$, is one of the most common antennas. The total length of the antenna represents half the wavelength of the emitted wave. This is basically what we have done just before, with some additional conditions, so we briefly go through this part. In particular, the time-dependent current can be written as:

$$I(x,y,z) = I_0 \sin\left(k(\frac{l}{2} - |z|)\right)\cos(\omega t) = I_0 \sin\left(\frac{\pi}{2} - k|z|\right))\cos(\omega t) = I_0 \cos(kz)\cos(\omega t)$$

for any $z \in [-l/2, l/2]$.

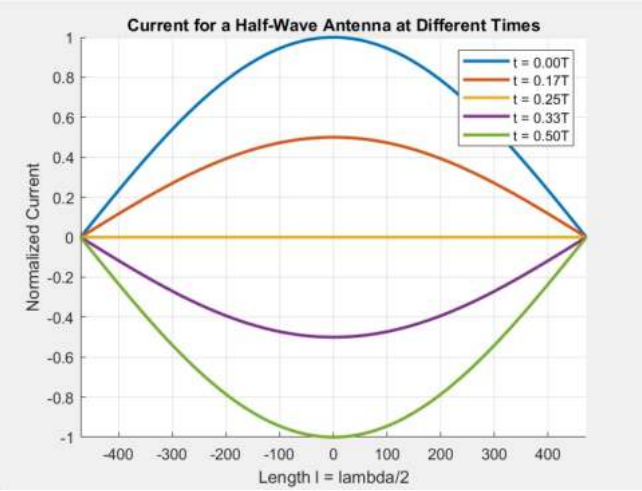

Figure 8: Current in a Half-Wave antenna ($l = \lambda/2$) at different times using $I(z) = I_0 \sin\big(k(\frac{l}{2} - |z|)\big)\cos(\omega t)$

We also rewrite the electromagnetic fields which will be needed later on:

$$\vec{E} = -i\eta\frac{e^{-ikr}}{2\pi r}\frac{I_0}{\sin\theta}\cos\left(\cos\theta\frac{kl}{2}\right)\cos(\omega t)\vec{e}_\theta, \qquad \vec{H} = -i\frac{e^{-ikr}}{2\pi r}\frac{I_0}{\sin\theta}\cos\left(\cos\theta\frac{kl}{2}\right)\cos(\omega t)\vec{e}_\phi$$

Since $\cos\big(\frac{kl}{2}\big) = \cos\big(\frac{\pi}{2}\big) = 0$, the radiation intensity is then given by:

$$\boxed{U(\theta) = \frac{\eta}{8\pi^2}\frac{|I_0|^2}{\sin^2\theta}\left[\cos\left(\cos\theta\frac{\pi}{2}\right)\right]^2}$$

which was numerically solved in the previous section.

5
ANTENNA ARRAYS

This section introduces antenna arrays and array design methods, demonstrating how multiple antennas can be combined to control and optimize the overall radiation pattern.

5.1 Uncoupled Antenna Arrays

In this section, we will build antenna arrays based on the two antennas studied previously. We are assuming identical linear wire antennas aligned with the z-axis centered at any position (x_n, y_n, z_n) and we neglect their radius when looking at the far-field.

Antenna arrays may be formed by considering a group of antenna elements, such as small or half-wave dipoles, arranged in particular geometrical configurations, such as along a particular direction. Some examples of antenna arrays that are made up from identical antenna elements are as follows.

$$\mathbf{j}(\mathbf{r}) = \hat{\mathbf{z}} \sum_n a_n I(z)\delta(x - x_n)\delta(y) \qquad \text{array along } x\text{-direction}$$

$$\mathbf{j}(\mathbf{r}) = \hat{\mathbf{z}} \sum_n a_n I(z)\delta(y - y_n)\delta(x) \qquad \text{array along } y\text{-direction}$$

$$\mathbf{j}(\mathbf{r}) = \hat{\mathbf{z}} \sum_n a_n I(z - z_n)\delta(x)\delta(y) \qquad \text{array along } z\text{-direction}$$

$$\mathbf{j}(\mathbf{r}) = \hat{\mathbf{z}} \sum_{mn} a_{mn} I(z)\delta(x - x_m)\delta(y - y_n) \qquad \text{2D planar array}$$

The weights a_n, a_{mn} are complex coefficients that represent both the amplitude and phase of the signal fed to the n^{th} antenna element. They are chosen appropriately to achieve desired directivity properties for the array. In practice, antenna array weights are applied using phase shifters and attenuators in analog systems or digitally through signal processing in digital systems.

The current density vector will be zero everywhere, except at the antenna positions $\mathbf{d_n} = (x_n, y_n, z_n)$. The current density of each individual translated antenna will be $\mathbf{j_d}(\mathbf{r}) = \mathbf{j}(\mathbf{r} - \mathbf{d})$. And thus the radiation vector of the translated current being the three-dimensional Fourier transform of the current density, yields

$$\mathbf{F}_d = \int e^{j\mathbf{k}\cdot\mathbf{r}} \mathbf{j}(\mathbf{r} - \mathbf{d}) d^3\mathbf{r} \tag{25}$$

$$= \int e^{j\mathbf{k}\cdot(\mathbf{r}'+d)} \mathbf{j}(\mathbf{r}') d^3\mathbf{r}' \tag{26}$$

$$= e^{j\mathbf{k}\cdot\mathbf{d}} \int e^{j\mathbf{k}\cdot\mathbf{r}'} \mathbf{j}(\mathbf{r}') d^3\mathbf{r}' \tag{27}$$

$$= e^{j\mathbf{k}\cdot\mathbf{d}} \mathbf{F} \tag{28}$$

where $\mathbf{F}$ was defined for a single antenna with current density $\mathbf{j}(\boldsymbol{r})$ placed at the origin.
Extending this translational phase shift to a three dimensional array of several identical antennas at various positions with respective relative feed coefficients we obtain the current of the n-th antenna to be $\mathbf{j}_n(\mathbf{r}) = a_n \mathbf{j}(\mathbf{r} - \mathbf{d}_n)$ and the corresponding radiation vector $\mathbf{F}_n(k) = a_n e^{j\mathbf{k}\cdot\mathbf{d}_n} \mathbf{F}(\mathbf{k})$

We then deduce that the total current density is:

$$\mathbf{j}_{tot} = \sum_{i=0}^{n} a_i \mathbf{j}(\mathbf{r} - \mathbf{d}_i)$$

And by the principle of superposition, the total radiation vector is:

$$\mathbf{F}_{tot}(\mathbf{k}) = \sum_{i=0}^{n} \mathbf{F}_i = \sum_{i=0}^{n} a_i e^{j\mathbf{k}\cdot\mathbf{d}} \mathbf{F}(\mathbf{k})$$

For this last equation we can obtain an array factor $A(\mathbf{k})$ such that:

$$\mathbf{F}_{tot}(\mathbf{k}) = A(\mathbf{k})\mathbf{F}(\mathbf{k})$$

And thus

$$A(\mathbf{k}) = \sum_{i=0}^{n} a_i e^{j\mathbf{k}\cdot\mathbf{d}}$$

Since $\mathbf{k} = k\hat{\mathbf{r}}$, we can write the array factor as $A(\hat{\mathbf{r}})$ or even $A(\theta, \phi)$ to show the orientation dependence. The radiation intensity can be computed easily:

$$\boxed{U_{tot}(\theta, \phi) = \big|A(\theta, \phi)\big|^2 U(\theta, \phi)} \tag{29}$$

Now, the radiation intensity is composed of two terms:

- $U(\theta, \phi)$ is the radiation intensity of a single antenna. This term is intrinsic to the type antenna used to build the array. We have studied dipoles and standing waves antennas, but there exists many others.
- $\big|A(\theta, \phi)\big|$ which is of great interest for this part. It will shape the radiation pattern in the xy-plane due to the ϕ dependence. For the following 2D graphs, we will now focus on $A(\theta = \pi/2, \phi) = A(\phi)$ where we expect the highest directivity.

5.1.1 • Uniform Arrays

We now look at a *uniform* array composed of N isotropic elements distributed along the x-axis with constant spacing d.

By definition, all weights are equal in a uniform array. We define the weight list:

$$\mathbf{a} = [a_0, ..., a_{N-1}] = \frac{1}{N} \times [1, 1, ...1]$$

The corresponding array factor:

$$A(z) = \frac{1}{N}\sum_{i=0}^{n} z^i = \frac{1}{N}\frac{z^N - 1}{z - 1} \implies A(\phi) = \frac{1}{N}\sum_{i=0}^{n} e^{ji\psi} = \frac{1}{N}\frac{e^{jN\psi} - 1}{e^{j\psi} - 1}$$

Where we substituted z for $e^{j\psi}$ and $\psi = kdcos(\phi)$ for an array along the x-axis, and we are looking at the direction on the xy-plane.

We can then rewrite for a uniform array:

$$A(\psi) = \frac{sin(\frac{N\psi}{2})}{Nsin(\frac{\psi}{2})} e^{j(N-1)\psi/2}$$

We can have a look at a first example with the 3D radiation pattern on Figure 9. We already see a huge enhancement compared to the radiation pattern of a single antenna.

We will now vary various parameters to observe how the pattern is evolving. As discussed above, we are mostly interested in $|A(\theta = \pi/2, \phi)|^2$ which is the normalized power pattern that arises solely from the array's geometry such as spacing, number of elements under the assumption that the individual elements are isotropic point sources. In short, it is more relevant to plot only $|A(\theta, \phi)|^2$ to get a better understanding of the array's structure for further optimization.

Let us see below how the pattern is changing with **increasing spacing** between elements in the arrays.

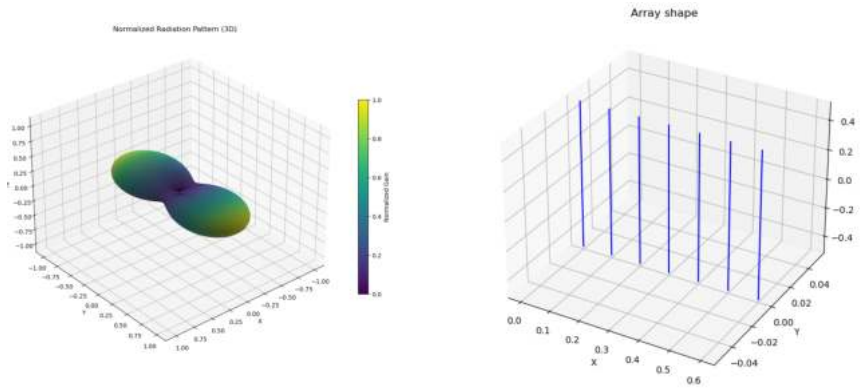

Figure 9: 3D radiation pattern, $N = 7$ and a constant spacing $d = 0.1\lambda$, Standing wave antenna

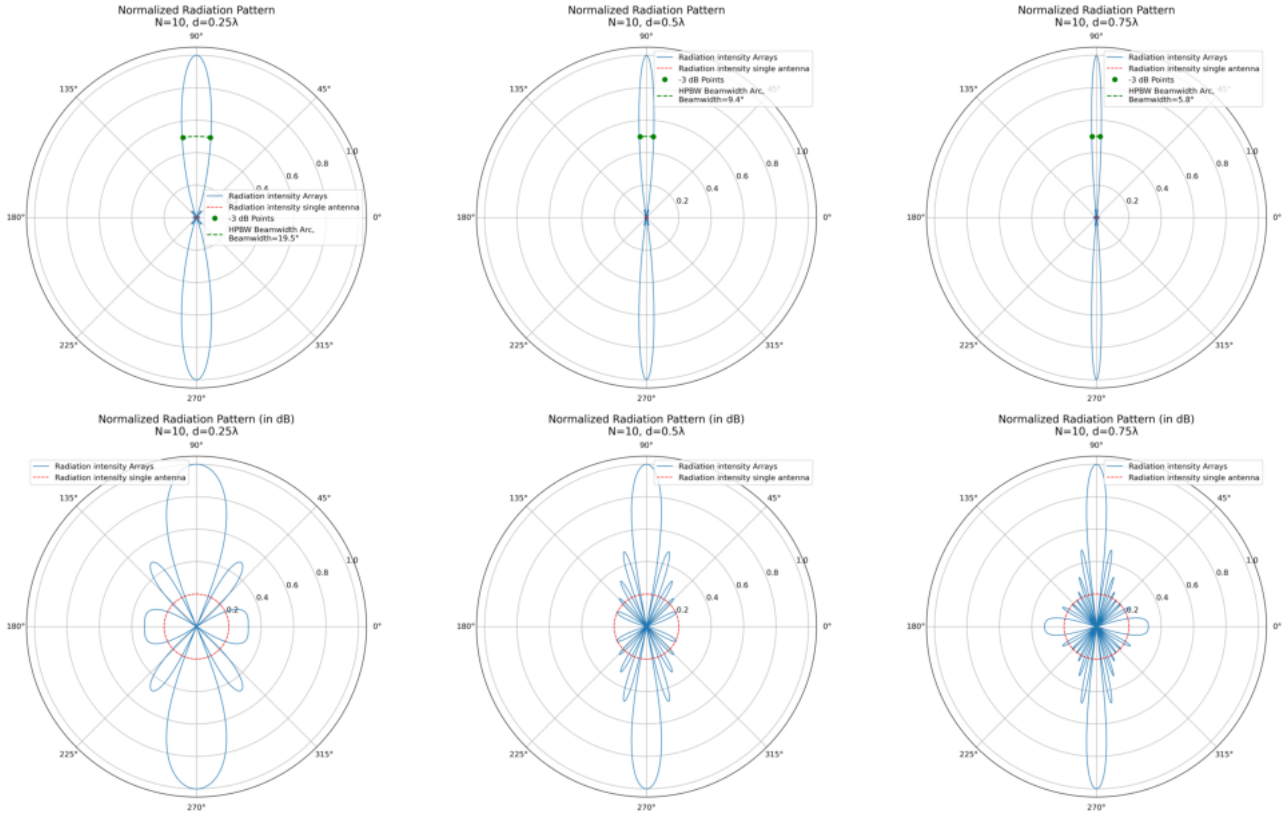

Figure 10: Normalized radiation intensity (in W and in dB) versus the azimuthal angle ϕ for a *uniform array* of 10 dipoles, with varying spacing from $d = 0.25\lambda$ to $d = 0.75\lambda$. Note that these radiation patterns were obtained from an Array of $N = 10$ dipoles, but we obtain exactly the same pattern for standing wave antennas because the type of antenna affects the variation with θ.

As usual, we provide the Python codes for Figures 10 here and our Github repository can be found in the Appendix.

Observations:
As can be seen in Figure 10, the normalized radiation pattern varies depending on the distance placed between

two antennas. This aligns with the theory, because the spacing will affect the de-phasing between each wave, emitted by each element in the array. This will create constructive interferences in some directions, and destructive in others, which is exactly what we want to refine. Notice that increasing the distance in units of lambda between two antenna's increases the directivity of the array in the direction perpendicular to the x axis. Analysing the figures above, we observe that the beamwidth is decreased as the distance d in units of lambda between two antennas is increased. We see that for $d = 0.25\lambda$ the beam width is of 25.3°, whereas for $d = 0.75\lambda$, the beam width is of 7.9°. Array's with shorter spacings thus have broader main lobes which make them suitable for wide coverage although not having good spatial resolution. Alternatively, the larger the distance in the array, the better the spatial resolution and the main lobe is thinner meaning a thin coverage. Notice that in the the radiation pattern of for a spacing between two antenna's the directivity along the perpendicular access is the best out of all of our plots. However two lobes are present along the array axis (i.e. 180° axis), these are grating lobes. This grating happens for $d \geq \lambda$, and in practice disturbs the signal received by the antenna as it perceives unequally strong signals to be equally strong.

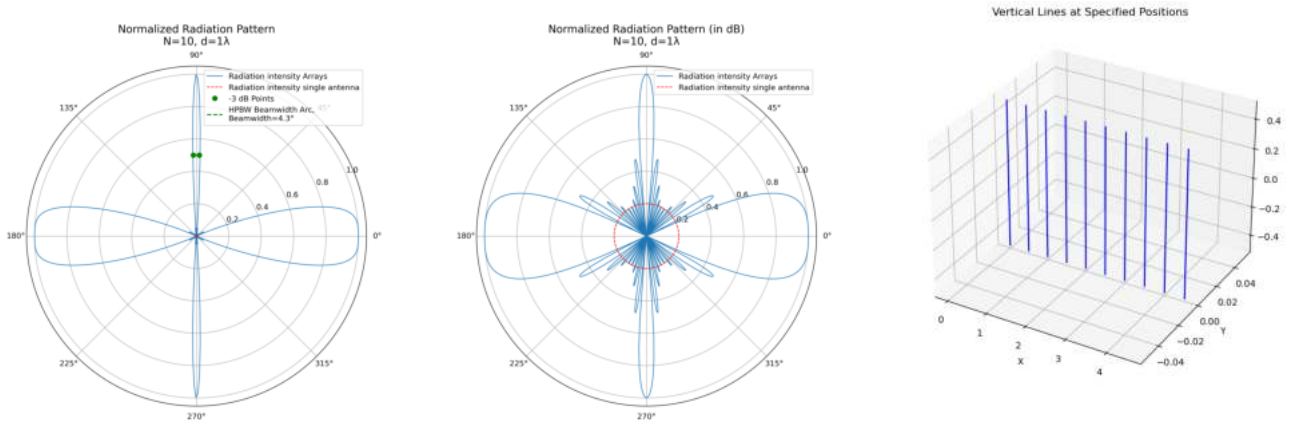

Figure 11: Normalized radiation intensity (in W and in dB) versus the azimuthal angle ϕ for a *uniform array* of 10 dipoles fixed spacing $d = \lambda$.

Interestingly, we can observe the strong decrease in beamwidth, i.e. an increase in directivity D with an **increasing number of elements**:

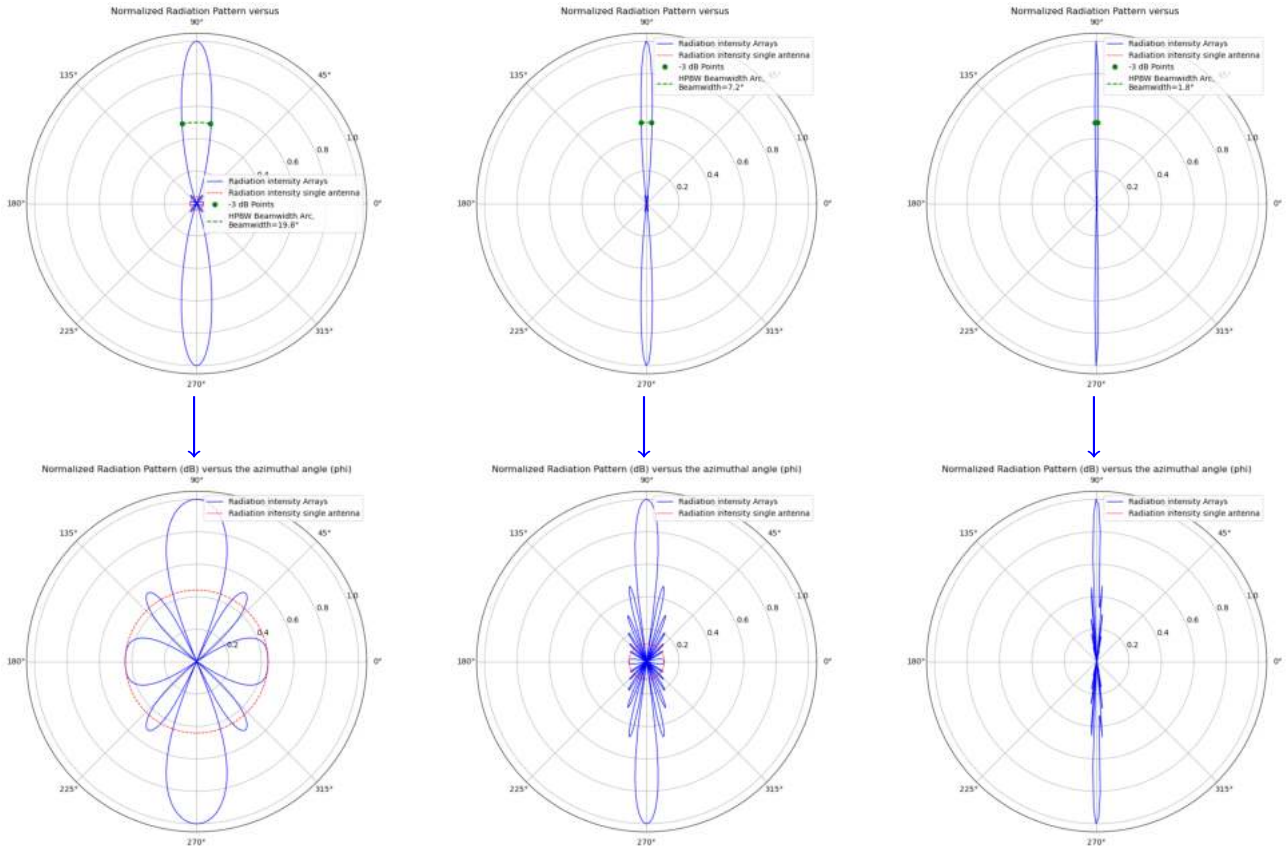

(a) $N = 5$, Beamwidth $= 19.8°$ (b) $N = 13$, Beamwidth $= 7.2°$ (c) $N = 40$, Beamwidth $= 1.8°$

Figure 13: Normalized radiation intensity (in W and in dB) versus the azimuthal angle ϕ for a *uniform array* of varying number of half-wave antenna with fixed spacing $d = 0.5\lambda$. The red curve emphasizes the high directivity gain in specific directions $\phi = \pi/2, 3\pi/2$ in comparison to a single half-wave antenna emitting isotropically by rotation around the z-axis.

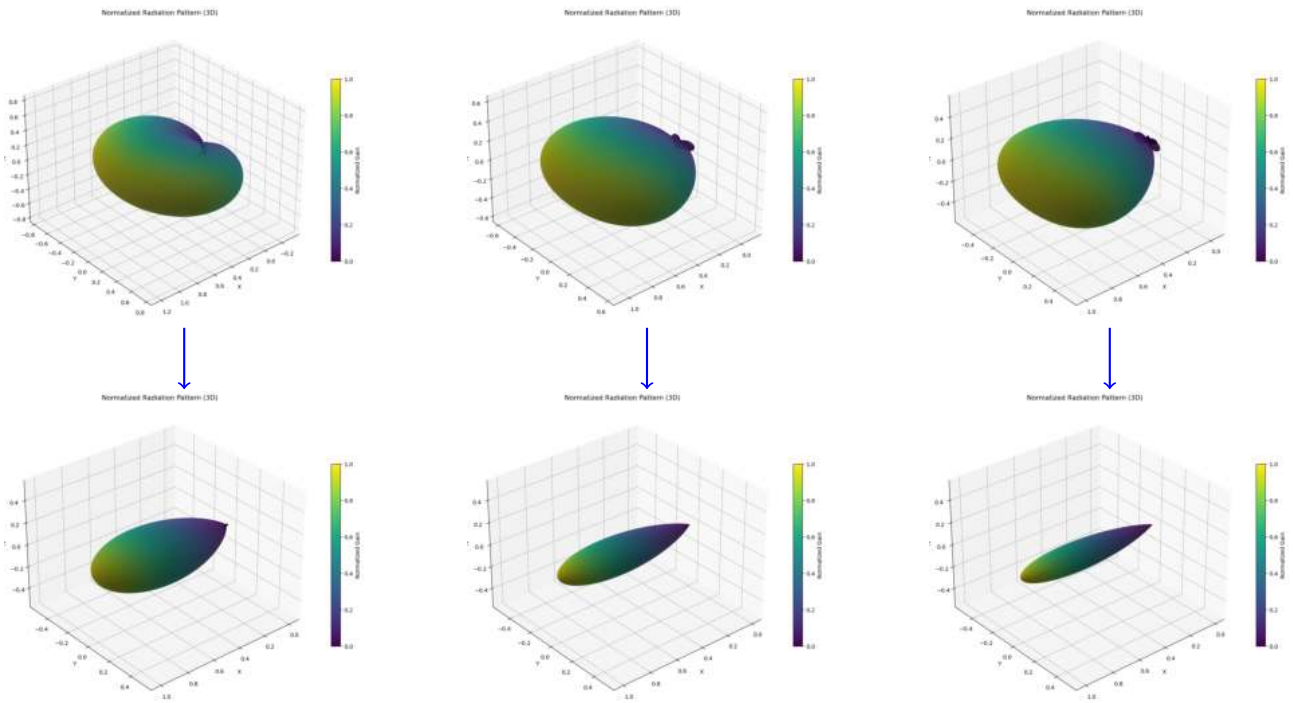

Figure 15: Directivity for a *uniform array* of N dipoles and $d = \lambda/10$, vs Schelkunoff's zero-placement with N = 5,10,15

Observations:

- Increasing the number of antennas in the array improves directivity.
- In practice, the size of the array that we can actually build may be constrained.

Since our code works for an arbitrary array made of parallel antennas, we can consider other possible antenna array configurations over a 2D plane. Below we illustrate some interesting plots, with for instance high directivity is several direction, improving the quality of the signal in every of these directions:

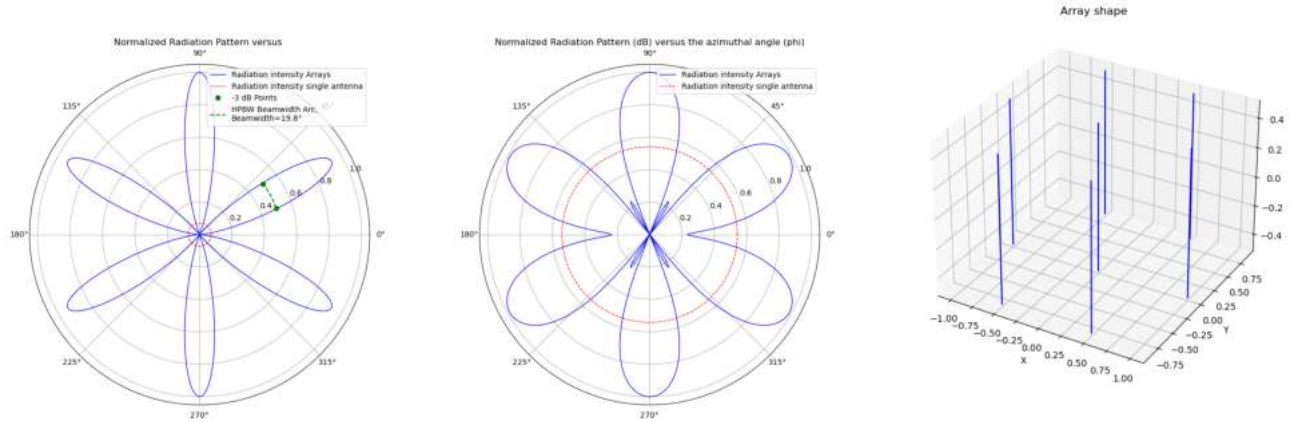

Figure 16: Example of triangular array with weights and positions that yield a clean, high-directivity beam in different directions

5.2 Visible region, Nyquist interval, and suitable element spacing

We are now going to investigate various concepts that will enable the enhancement of arrays directivity.

For a linear array lying on the x-axis the spatial frequency is

$$\psi = k\,d\,\cos\phi, \qquad k = \frac{2\pi}{\lambda},\ 0 \le \phi < 2\pi,$$

so ψ varies over the *visible region*

$$-kd \ \le\ \psi \ \le\ kd.$$

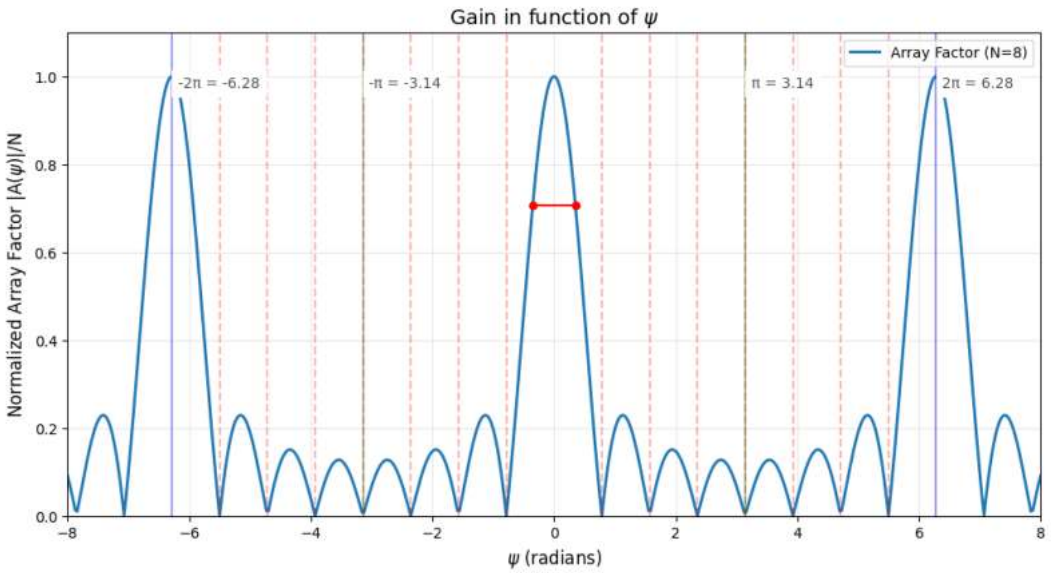

Figure 17: Normalized array gain as a function of direction.

Because the array factor $A(\psi)$ is periodic with period 2π, we may study it on any interval of length 2π; the standard choice $-\pi < \psi < \pi$ is the *first Nyquist interval*. Comparing the width of the visible region to this $\pm\pi$ window leads to three regimes:

(i) $\boldsymbol{kd \le \pi}$ $\boldsymbol{(d \le \lambda/2)}$
The entire visible band fits within one Nyquist interval; hence the pattern exhibits a single main lobe (and its symmetric counterpart) with relatively few sidelobes.

(ii) $\boldsymbol{\pi < kd < 2\pi}$ $\boldsymbol{(\lambda/2 < d < \lambda)}$
The visible band spills partly into neighbouring Nyquist intervals. A portion of the spectrum repeats, so the pattern is theoretically aliased; independent specification of $\boldsymbol{A(\psi)}$ in the overlapping zones would be inconsistent (overspecification), but grating lobes have not yet appeared in the visible sector.

(iii) $\boldsymbol{kd \ge 2\pi}$ $\boldsymbol{(d \ge \lambda)}$
The visible region $\boldsymbol{-kd \le \psi \le kd}$ covers two or more complete Nyquist intervals. Consequently, grating lobes—main-beam–strength replicas—emerge within the visible field.

Design rules

- To *prevent grating lobes*, keep the first spectral replica outside the visible region:

$$kd < 2\pi \quad \Longleftrightarrow \quad d < \lambda.$$

- To *eliminate aliasing altogether*, ensure the visible region stays within a single Nyquist window:

$$kd \leq \pi \quad \Longleftrightarrow \quad d \leq \tfrac{\lambda}{2},$$

  which is equivalent to the spatial sampling theorem condition $1/d \geq 2/\lambda$.

5.3 Rotation

Now suppose we have tailored an antenna array with a focused, sharp beam in one direction. The problem is how to steer the beam without rebuilding the entire setup, which can be tedious and difficult to reproduce.

One solution is *array steering*: we shift

$$A(\psi) \longrightarrow A(\psi - \psi_0)\,.$$

Since

$$A(\psi) = \sum_n a_n\, e^{jn\psi},$$

we obtain

$$A(\psi - \psi_0) = \sum_n a_n\, e^{jn(\psi-\psi_0)} = \sum_n \left(a_n e^{-jn\psi_0}\right) e^{jn\psi}\,,$$

so each weight is multiplied by the phase factor $e^{-jn\psi_0}$. In a uniform array ($a_n = 1$) one simply sets

$$a_n = z^n, \quad z = e^{-j\psi_0}\,.$$

To steer the main beam to an angle ϕ (measured from the array axis), convert to radians:

$$\phi_0 = \phi\frac{\pi}{180},$$

and then compute

$$\psi_0 = k\,d\cos\phi_0.$$

Figure 15 shows examples of the resulting rotated patterns.

We observe that these steered patterns are no longer symmetric about $\psi = 0$; originally the pattern was symmetric about broadside, but after steering the symmetry is preserved only about the array axis. Indeed, the main lobes satisfy

$$\psi - \psi_0 = 2\ell\pi,$$

which, since $\psi = kd\cos\phi$, gives

$$\cos\phi - \cos\phi_0 = \frac{2\ell\pi}{k\,d} \quad \Longrightarrow \quad \cos\phi = \cos\phi_0 + \frac{2\ell\pi}{k\,d}.$$

Here $2\ell\pi$ corresponds to any multiple of 2 pi contained in the new interval $[-kd(1+cos(\psi_0)),\ kd(1-cos(\psi_0)]$. For $\ell = 0$ one finds

$$\phi = \phi_0 \quad \text{or} \quad \phi = -\phi_0,$$

while for $\ell > 0$ the additional solutions likewise come in symmetric pairs, by the periodicity of the cosine function. Consequently, there are precisely twice the number of Nyquist intervals in grating lobes, corresponding to

$$m \;=\; 2\frac{\psi_{\text{vis}}}{2\pi} \;=\; \frac{2kd}{\pi} \;=\; \frac{4d}{\lambda}.$$

Find below two plots that illustrate the rotation for $\phi_0 = 45°$ and $\phi_0 = 30°$ and one showing the grating lobes.

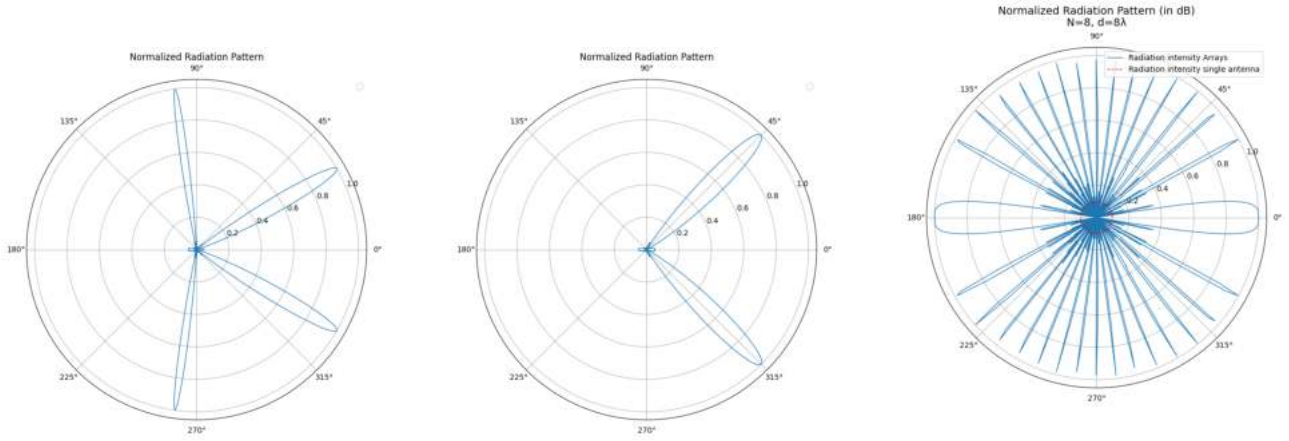

Figure 18: Normalized radiation intensity (in dB) versus the azimuthal angle ϕ for a *uniform array* of 10 dipoles with $d = \lambda$, $\phi_0 = 30°$, and $d = \lambda/2$, $\phi_0 = 45°$.

Note that steering does not rigidly rotate the directivity pattern: the beamwidth and sidelobe levels generally change, since the gain maxima now occur at the angles ϕ determined above.

5.3.1 • Optimization

We've seen how to build a uniform array and confronted ourselves with the problem of choosing different values of d, each of which has advantages and disadvantages. We will now study how we can further optimise the directivity.

There exist various methods to design arrays effectively, and we will focus on Schelkunoff's zero-placement method, which is particularly useful when $d < \lambda/2$. It consists of displacing the zeros of $A(\psi)$ so that they all lie in the visible region, which is not the full circle because $kd < \pi$. The more zeros we place in the visible region, the narrower our main lobes become and the sidelobes are significantly reduced.

To achieve this, we first rotate the directivity pattern to 0 rad so that the calculations are easier. We then find the polynomial A whose roots are evenly spaced in the interval $[-2kd, 0]$ using NumPy's polynomial functions. From the polynomial A we adjust the weights and finally plot the resulting patterns :

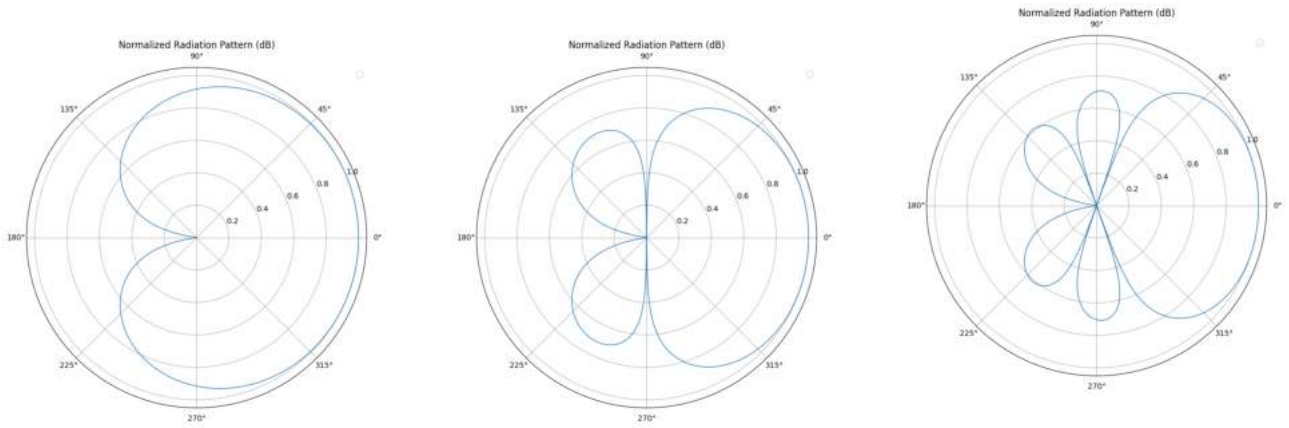

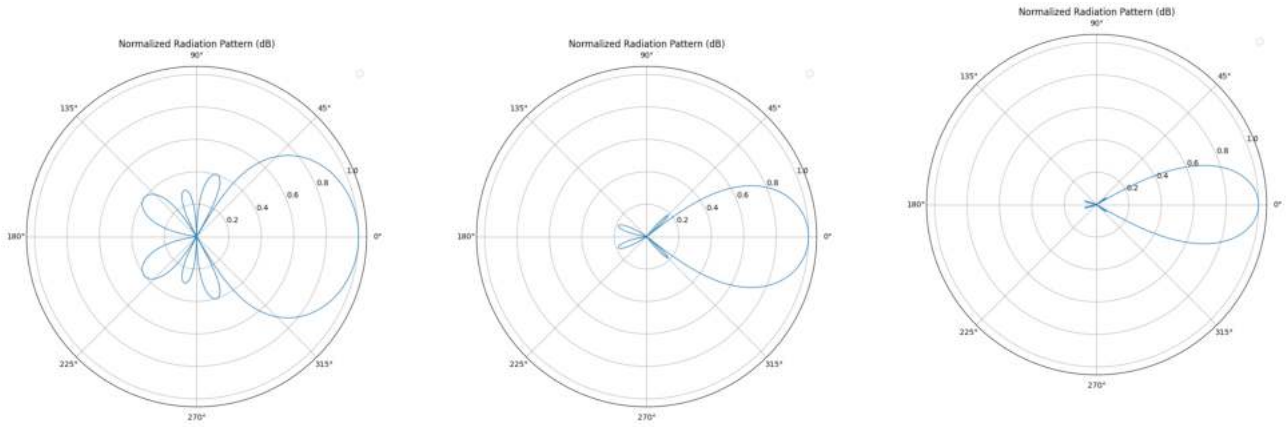

Figure 20: Directivity for a *uniform array* of N dipoles and $d = \lambda/10$,vs Schelkunoff's zero-placement with N = 5,10,15

The upper panels illustrate the radiation patterns of the uniform array under the specified conditions, while the lower panels show the corresponding patterns after applying Schelkunoff's zero-placement optimization using the same element spacings and steering angles. By relocating the zeros of the array factor so that they lie strictly within the visible region, the optimized array produces a noticeably sharper main lobe, greatly suppressed sidelobes, and correspondingly lower wasted power outside the beam.

So far, we have concentrated primarily on the analysis and design of antennas. In the analysis problem an antenna model is chosen, and it's radiation characteristics (pattern, directivity, beam width and efficiency) are analysed. This is usually accomplished by initially specifying the current distribution of the antenna, and then analysing it using standard procedures. What if only one antenna among others is fed? Will this have some effect on nearby antennas? What role will the parasitic elements play in the overall performance of the antenna system?

5.4 Coupled Antennas

In this section, we aim to quantify the proximity interactions between parallel thin wire antennas which was neglected so far. We shall see that when a voltage is applied to one antenna, it generates an electromagnetic field that induces currents in nearby antennas. These induced currents, in turn, affect the original antenna, an effect known as *mutual impedance*. Additionally, each antenna influences itself through its own radiated field, a phenomenon referred to as *self-impedance*.

We first analyze the influence between a coupled two-element arrays. Then, we easily generalize to the case of an arbitrary array of parallel linear antennas.

5.4.1 • Two Elements

We assume that the (z-directed) dipoles are center-driven by the voltage generators V_1,V_2. Let $I_1(z)$, $I_2(z)$ be the currents induced on the dipoles by the generators and by their mutual interaction, and let $h_1 = l_1/2$, $h_2 = l_2/2$ be the half-lengths of the antennas, and a_1, a_2 their radii (which is not zero unlike the far-field analysis since it has a relatively important effect). Then, assuming the thin-wire model, the total current density will have only a z-component given by (we ignore again the time dependent term $\cos(\omega t)$ as it doesn't affect the following calculations):

$$J_z(x, y, z) = I_1(z)\delta(x - x_1)\delta(y - y_1) + I_2(z)\delta(x - x_2)\delta(y - y_2)$$

with I_1 and I_2 the current in antenna-1 and antenna-2 respectively. From eq.20 (see thin wire antenna section), it follows that the vector potential in cylindrical coordinates is :

$$\boldsymbol{A}(z,\boldsymbol{\rho}) = A_z(z,\boldsymbol{\rho})\boldsymbol{e}_z = \frac{\mu_0}{4\pi}\boldsymbol{e}_z \int \frac{e^{-jkR}}{R} J_z(x',y',z')dx'dy'dz'$$

where $\boldsymbol{\rho} = x\boldsymbol{e}_x + y\boldsymbol{e}_y$ is the cylindrical radial vector and $R = |\boldsymbol{r} - \boldsymbol{r}'|$. Inserting the current density $J_z(x,y,z)$ and performing the x', y' integrations, we obtain:

$$A_z(z,\boldsymbol{\rho}) = \frac{\mu_0}{4\pi}\int_{-h_1}^{h_1} \frac{e^{-jkR_1}}{R_1} I_1(z')dz' + \frac{\mu_0}{4\pi}\int_{-h_2}^{h_2} \frac{e^{-jkR_2}}{R_2} I_2(z')dz'$$

where, R_1, R_2 are the distances from the z' point on each antenna to the (x,y,z) observation point, that is,

$$R_1 = \sqrt{(z-z')^2 + (x-x_1)^2 + (y-y_1)^2} = \sqrt{(z-z')^2 + |\boldsymbol{\rho} - \mathbf{d}_1|^2}$$
$$R_2 = \sqrt{(z-z')^2 + (x-x_2)^2 + (y-y_2)^2} = \sqrt{(z-z')^2 + |\boldsymbol{\rho} - \mathbf{d}_2|^2}$$

where $\mathbf{d}_1 = (x_1, y_1)$ and $\mathbf{d}_2 = (x_2, y_2)$ are the xy-locations of the antenna centers. According to eq.10, the z-component of the electric field generated by the two antenna currents will be:

$$j\omega\epsilon_0\mu_0 E_z(z,\boldsymbol{\rho}) = (\partial_z^2 + k^2)A_z(z,\boldsymbol{\rho}) \quad \text{ or } j\omega\frac{1}{c^2}E_z(z,\boldsymbol{\rho}) = jk\frac{1}{c}E_z(z,\boldsymbol{\rho}) = (\partial_z^2 + k^2)A_z(z,\boldsymbol{\rho})$$

We see that in terms of units,

$$[A_z]\cdot\frac{1}{[L]^2} = \frac{1}{[T]}\cdot\frac{[T]^2}{[L]^2}\cdot\frac{[Voltage]}{[L]} \implies [cA_z] = [Voltage]$$

Working with the rescaled scalar potential $V(z,\boldsymbol{\rho}) = 2jcA_z(z,\boldsymbol{\rho})$, we rewrite:

$$V(z,\boldsymbol{\rho}) = \frac{j\eta}{2\pi}\int_{-h_1}^{h_1} \frac{e^{-jkR_1}}{R_1} I_1(z')dz' + \frac{j\eta}{2\pi}\int_{-h_2}^{h_2} \frac{e^{-jkR_2}}{R_2} I_2(z')dz'$$

$$(\partial_z^2 + k^2)V(z,\boldsymbol{\rho}) = -2kE_z(z,\boldsymbol{\rho}) \tag{30}$$

Denoting by $V_1(z) = V(z, \sqrt{x_1^2 + y_1^2})$ and $V_2(z) = V(z, \sqrt{x_2^2 + y_2^2})$ the values of $V(x,y,z)$ on the surfaces of antenna-1 and antenna-2, we obtain from above:

$$V_1(z) = V_{11}(z) + V_{12}(z)$$
$$V_2(z) = V_{21}(z) + V_{22}(z)$$

The z-components of the electric fields induced on the surfaces of antenna-1 and antenna-2 are obtained by applying Eq.30 relating E_z to V:

$$E_{1z}(z) = E_1(z) = E_{11}(z) + E_{12}(z)$$
$$E_{2z}(z) = E_2(z) = E_{21}(z) + E_{22}(z)$$

where we defined, for $p, q = 1, 2$:

$$V_{pq}(z) = \frac{j\eta}{2\pi}\int_{-h_q}^{h_q} G_{pq}(z-z')I_q(z')dz' \tag{31}$$

$$(\partial_z^2 + k^2)V_{pq}(z) = -2kE_{pq}(z) \tag{32}$$

and the impedance kernels (or Green function):

$$G_{pq}(z-z') = \frac{e^{-jkR_{pq}}}{R_{pq}}, \quad R_{pq} = \sqrt{(z-z')^2 + d_{pq}^2}$$

Note that we are only concerned with the z-component of the electric field, as for a thin-wire antenna, this is the only component that contributes to the current along the antenna.

If $p \neq q$, then d_{pq} is the xy-distance between the antennas, and if $p = q$, it is the radius of the corresponding antenna, that is,

$$d_{12} = d_{21} = |\mathbf{d}_1 - \mathbf{d}_2| = \sqrt{(x_1-x_2)^2 + (y_1-y_2)^2}$$

$$d_{11} = a_1, \quad d_{22} = a_2 \tag{25.4.10}$$

In the first case, the antenna radius is neglected because it is typically much smaller than the distance between the two antennas. However, in the second case, the radius must be taken into account, as the antenna interacts with itself through its own physical size. There is also a mathematical reason for this: when $z - z' = 0$, neglecting the radius would lead to a division by zero.
Thus, $V_{pq}(z)$ and $E_{pq}(z)$ are the vector potential and the z-component of the electric field induced on antenna p by the current $I_q(z)$ on antenna q.

Now, the subtle part is to that, we are dealing with two thin-wire antennas, each excited precisely at their centers by a delta-gap source (which in practice is due to transmission lines arriving at the center). The delta-gap is a mathematical idealization of a localized voltage source, modeled by the delta-Dirac distribution. On the wire's surface, only the normal field is allowed. The total tangential electric field must be zero because a perfect conductor cannot support an electric field tangent to its surface in steady-state i.e. the charges rearrange to cancel it out. But the delta-gap generator adds a localized electric field at the feed point, so for the field to vanish on the wire, the wire must produce an equal and opposite field. Hence, on the surface of the first antenna, the electric field E_z must cancel the field of the delta-gap generator in order for the total tangential field to vanish, that is,

$$E_1(z) = -E_{1,\text{in}}(z) = -V_1\delta(z).$$

Similarly, on the surface of the second antenna, we must have

$$E_2(z) = -E_{2,\text{in}}(z) = -V_2\delta(z).$$

Let us now define the mutual (and self) impedance between antenna-p and antenna-q for $p, q = 1, 2$:

$$Z_{pq} = -\frac{1}{I_pI_q}\int_{-h_p}^{h_p} E_{pq}(z)I_p(z)\,dz$$

and, more explicitly:

$$Z_{11} = -\frac{1}{I_1I_1}\int_{-h_1}^{h_1} E_{11}(z)I_1(z)\,dz, \quad Z_{12} = -\frac{1}{I_1I_2}\int_{-h_1}^{h_1} E_{12}(z)I_1(z)\,dz$$

$$Z_{21} = -\frac{1}{I_2I_1}\int_{-h_2}^{h_2} E_{21}(z)I_2(z)\,dz, \quad Z_{22} = -\frac{1}{I_2I_2}\int_{-h_2}^{h_2} E_{22}(z)I_2(z)\,dz$$

Using these definitions, we find:

$$Z_{11}I_1 + Z_{12}I_2 = -\frac{1}{I_1}\int_{-h_1}^{h_1}[E_{11}(z) + E_{12}(z)]I_1(z)\,dz$$
$$= -\frac{1}{I_1}\int_{-h_1}^{h_1} E_1(z)I_1(z)\,dz \qquad = -\frac{1}{I_1}\int_{-h_1}^{h_1}[-V_1\delta(z)]I_1(z)\,dz = \frac{1}{I_1}V_1I_1(0) = V_1$$

where, by definition, $I_1(z=0) = I_1$. Similarly, for $p = 2$ we have:

$$Z_{21}I_1 + Z_{22}I_2 = V_2$$

or more concisely, in matrix notation:

$$\begin{bmatrix} Z_{11} & Z_{12} \\ Z_{21} & Z_{22} \end{bmatrix}\begin{bmatrix} I_1 \\ I_2 \end{bmatrix} = \begin{bmatrix} V_1 \\ V_2 \end{bmatrix} \Leftrightarrow \boldsymbol{ZI} = \boldsymbol{V}$$

The mutual impedance Z_{pq} actually satisfies the reciprocity symmetry condition, $Z_{pq} = Z_{qp}$, meaning that the impedance matrix written above is symmetric. To write it in a form that shows this condition explicitly, we replace $E_{pq}(z)$ by Eq.32:

$$E_{pq}(z) = \frac{-1}{2k}(\partial_z^2 + k^2)V_{pq}(z) = \frac{-j\eta}{4\pi k}\int_{-h_q}^{h_q} I_q(z')(\partial_z^2 + k^2)G_{pq}(z - z')dz'$$

and obtain the alternative symmetric form:

$$Z_{pq} = \frac{j\eta}{4\pi k}\int_{-h_p}^{h_p}\int_{-h_q}^{h_q}\frac{I_p(z)I_q(z')}{I_pI_q}(\partial_z^2 + k^2)G_{pq}(z - z')\,dz'\,dz$$

We will deal with almost half-wave antenna. If we assume that the currents are sinusoidal, that is, for $p = 1, 2$:

$$I_p(z) = I_p\frac{\sin(k(h_p - |z|))}{\sin(kh_p)} \tag{33}$$

with I_p to be determined. Then, in the expression of Z_{pq} the ratios $I_p(z)/I_p$ and hence Z_{pq} become independent of the input currents at the antenna terminals and depend only on the geometry of the antennas:

$$Z_{pq} = \frac{j\eta}{4\pi k}\int_{-h_p}^{h_p}\int_{-h_q}^{h_q}\frac{\sin(k(h_p - |z|))}{\sin(kh_p)}\frac{\sin(k(h_q - |z'|))}{\sin(kh_q)}(\partial_z^2 + k^2)G_{pq}(z - z')\,dz'\,dz \tag{34}$$

A further detailed calculation can be found in the appendix

Let us mention that instead of this assumption, one can also the decompose each antenna in N sections and discretize the current on the nth element in a set of known (chosen) basis functions such as a Fourier series expansion of the form: $\sum_{m=1}^{M} I_{nm}\cos\left[(2m-1)\frac{\pi z'}{l_n}\right]$. where I_{nm} represents the complex current coefficient of mode m on element n and l_n represents the corresponding length of the n element. M is the number of current modes. As explained in [1], this would lead to a system of N equations for each antenna. It turns out that the result remains approximately valid when considering a standing wave antenna that is close in length to a half-wavelength. However, it's important to note that the sinusoidal current assumption becomes less accurate as the antenna length deviates from the half-wavelength. For example, this assumption no longer holds for a full-wavelength antenna (the impedance coefficient in eq.46 would become infinite since we divide by $\sin(kh_p) = \sin(2\pi) = 0$). Nevertheless, such cases are beyond the scope of our present discussion.

5.4.2 • Generalization

The above results on two antennas generalize in a straightforward fashion to several antennas. This method is called the *Induced EMF Method*.
We consider N parallel antennas aligned along the z-axis in a side-by-side arrangement with centers at positions (x_p, y_p), and driving voltages, lengths, and radii V_p, l_p, a_p, where $p = 1, 2, \ldots, N$.

Assuming sinusoidal currents as previously $I_p(z) = I_p \frac{\sin(k(h_p - |z|))}{\sin(kh_p)}$, we define the mutual impedance coefficients Z_{pq} as in eq.46, where p, q take on the values $p, q = 1, 2, \ldots, N$.
For the sake of clarity, we rewrite them below (with $h_p = l_p/2$):

$$Z_{pq} = \frac{j\eta}{4\pi k} \int_{-h_p}^{h_p} \int_{-h_q}^{h_q} \frac{\sin(k(h_p - |z|))}{\sin(kh_p)} \frac{\sin(k(h_q - |z'|))}{\sin(kh_q)} (\partial_z^2 + k^2) G_{pq}(z - z')\, dz'\, dz \tag{35}$$

where

$$G_{pq}(z - z') = \frac{e^{-jkR_{pq}}}{R_{pq}}, \quad R_{pq} = \sqrt{(z - z')^2 + d_{pq}^2}$$

and the mutual distances (distance separating antenna-p from antenna-q) are:

$$d_{pq} = \begin{cases} a_p & \text{if } p = q \\ \sqrt{(x_p - x_q)^2 + (y_p - y_q)^2} & \text{if } p \neq q \end{cases}$$

As before, we have the crucial relationship between the unknown intensity and the (known) input voltage:

$$V_p = \sum_{q=1}^{N} Z_{pq} I_q \text{ for } p \in \{1, 2, ..., N\} \Leftrightarrow \boldsymbol{ZI} = \boldsymbol{V} \Leftrightarrow \begin{bmatrix} Z_{11} & Z_{12} & \cdots & Z_{1N} \\ Z_{21} & Z_{22} & \cdots & Z_{2N} \\ \vdots & \vdots & \ddots & \vdots \\ Z_{N1} & Z_{N2} & \cdots & Z_{NN} \end{bmatrix} \begin{bmatrix} I_1 \\ I_2 \\ \vdots \\ I_N \end{bmatrix} = \begin{bmatrix} V_1 \\ V_2 \\ \vdots \\ V_N \end{bmatrix} \tag{36}$$

We note that $\boldsymbol{Z}$ is a symmetric matrix, as a consequence of the reciprocity relations $Z_{pq} = Z_{qp}$.
Before going any further, let us simplify the expression of Z_{pq} using integration by parts twice:

$$\begin{aligned} Z_{pq} &= \frac{j\eta}{4\pi k} \int_{-h_p}^{h_p} \int_{-h_q}^{h_q} \frac{\sin(k(h_p - |z|))}{\sin(kh_p)} \frac{\sin(k(h_q - |z'|))}{\sin(kh_q)} (\partial_z^2 + k^2) G_{pq}(z - z')\, dz'\, dz \\ &= \frac{j\eta}{4\pi k} \int_{-h_q}^{h_q} \frac{\sin(k(h_q - |z'|))}{\sin(kh_q)\sin(kh_p)} \left(\int_{-h_p}^{h_p} \sin(k(h_p - |z|))(\partial_z^2 + k^2) G_{pq}(z - z') dz \right) dz' \end{aligned}$$

Which yields:

$$\begin{aligned} Z_{pq} &= \frac{j\eta}{4\pi k} \int_{-h_q}^{h_q} \frac{\sin(k(h_q - |z'|))}{\sin(kh_q)\sin(kh_p)} \left(kG_{pq}(-h_p - z') + kG_{pq}(h_p - z') - 2k\cos(kh_p) G_{pq}(-z') \right) dz' \\ &= \frac{j\eta}{4\pi} \frac{1}{\sin(kh_q)\sin(kh_p)} \int_{-h_q}^{h_q} \sin(k(h_q - |z'|)) \left[G_{pq}(-h_p - z') + G_{pq}(h_p - z') - 2\cos(kh_p) G_{pq}(-z') \right] dz' \end{aligned}$$

If we plot the integrand, we see that it is a smooth function that can be integrated using the numerical method described in the Appendix, whereas the first expression of Z_{pq} that we had, involving a double integral is hard to integrate because the function is extremely peaked when $z \approx z'$.

Given the driving voltages V_p, Eq.36 may be solved numerically for the induced currents amplitude I_p by inverting the impedance matrix: $\boldsymbol{I} = \boldsymbol{Z}^{-1}\boldsymbol{V}$. The reader can find the access to our detailed Python code for computing the impedance coefficients and matrix here. In short, *Z_new* is computing the mutual impedance given p, q as input. Based on this, *matrixZ_new* is returning the impedance matrix and given the input voltage in each antenna in a list V, *input_current* returns the current amplitude I_p.

This completely define the assumed sinusoidal currents $I_p(z)$. Then, from the knowledge of the currents $I_p(z)$, one can obtain the radiation pattern of the array, which we are going to derive in the next part.

5.4.3 • Far-field pattern

According to Eq.2.3, since the current density $\boldsymbol{J}$ is along the antenna axis $\hat{z}$, the radiation vector $\vec{F} = \hat{z}F_z$ has only a z-component given by:

$$F_z(\theta,\phi) = \int_V J_z(\vec{r}')e^{j\vec{k}\cdot\vec{r}'}d\vec{r}' \tag{37}$$

implying that:

$$\mathbf{F}_\perp = \hat{\theta}F_z(\theta,\phi)\sin\theta$$

Hence, the radiation fields are obtained from the final result of the far-field section, that is,

$$\vec{E} = \hat{\theta}E_\theta = \hat{\theta}jk\eta\frac{e^{-jkr}}{4\pi r}F_z(\theta,\phi)\sin\theta \tag{38}$$

$$\vec{H} = \hat{\phi}H_\phi = \hat{\phi}jk\frac{e^{-jkr}}{4\pi r}F_z(\theta,\phi)\sin\theta \tag{39}$$

But, in the thin-wire approximation, the total current density of the array is:

$$J_z(\vec{r}') = \sum_{p=1}^{N} I_p(z')\delta(x'-x_p)\delta(y'-y_p)$$

with (x_p, y_p) the position of antenna-p in the plane $z = 0$. Inserting this into Eq.37 and performing the x', y' integrations using the properties of delta-Dirac function, we obtain:

$$F_z(\theta,\phi) = \sum_{p=1}^{N} e^{jkx_p\sin\theta\cos\phi + jky_p\sin\theta\sin\phi}\int_{-h_p}^{h_p} I_p(z')e^{jkz'\cos\theta}dz'$$

Using Eq.45 for $I_p(z)$ and replacing $k_z = k\cos\theta$, we solve directly the integral according to Eq.24:

$$F_z(\theta,\phi) = \sum_{p=1}^{N} e^{jkx_p\sin\theta\cos\phi + jky_p\sin\theta\sin\phi}\frac{2I_p}{k\sin(kh_p)}\frac{\cos(kh_p\cos\theta)-\cos(kh_p)}{\sin^2\theta}$$

The average Poynting vector is easily computed:

$$\mathbf{\Pi} = \frac{1}{2}\boldsymbol{E}\times\boldsymbol{H}^* = \frac{1}{2}E_\theta H_\phi^*(\hat{\theta}\times\hat{\phi}) = \frac{k^2\eta}{2\cdot 16\pi^2 r^2}\left|\sin\theta\cdot F_z(\theta,\phi)\right|^2\hat{r}$$

Multiplying by r^2 gives the radiation intensity:

$$U(\theta,\phi) = \frac{\eta k^2}{32\pi^2}\left|\sin\theta\cdot F_z(\theta,\phi)\right|^2$$

More explicitly, we obtain:

$$\boxed{U(\theta,\phi) = \frac{\eta}{8\pi^2}\left|\sum_{p=1}^{N} I_p\frac{\cos(kh_p\cos\theta)-\cos(kh_p)}{\sin(kh_p)\sin\theta}e^{jk(x_p\cos\phi+y_p\sin\phi)\sin\theta}\right|^2} \tag{40}$$

5.5 Yagi-Uda Antenna

While the calculations detailed previously apply for any arrays of parallel dipole, with arbitrary parasitic ($V_p = 0$) and driven ($V_p = 1$) elements, we decided to focus on a very particular array called the Yagi-Uda antenna. This will constitute the core of our project. It involved everything we have seen so far: concepts such

as *directivity*; *impedance* as well as important numerical methods ...etc. The Yagi-Uda array is quite popular because it offers a strong directional signal while being relatively simple and inexpensive to build. Good directivity characteristics enhance the signal quality is one direction and are realized with certain choices for the antenna lengths and separations. This will be developed in the next section.

The Yagi-Uda antenna is composed of z-directed dipoles that are arranged along the x-axis. The second dipole is driven; all others are parasitic, meaning that they are not fed, they are passive elements, which only respond to the near external electromagnetic field. In particular, the first antenna is parasitic and acts as a reflector, i.e. it "sends back" the field coming from the driven element in order to increase the directivity in the positive x direction. Also, the elements to the right of the driven dipole have lengths slightly shorter, and act as “directors.” They accentuate the field of the driven element forward.

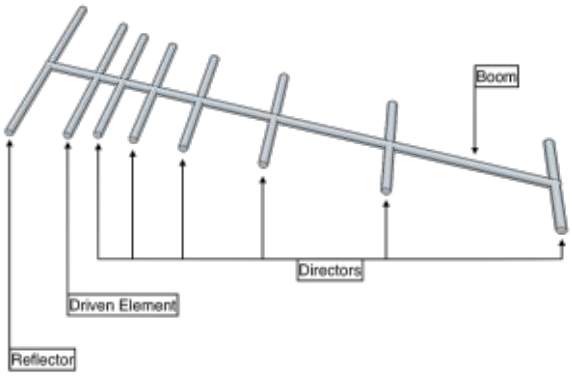

Figure 21: Yagi-Uda diagram with 8 elements. The typical form for a N elements Yagi antenna is in the following order: 1 reflector, 1 driven element, $N-2$ directors.

We now have all the tools to proceed: First we compute the current in each antenna thanks to Eq.36, knowing that $\boldsymbol{V} = [0, 1, 0, 0, ..., 0]^T$. Then we directly get the radiation intensity with Eq.40 and $y_p = 0$ for every p. However, we shall see that the resulting pattern and directivity can deviate from the expectation if the array is not optimized.

5.6 Discussion and Optimization of Directivity of the Yagi

We play the same game as Cheng and Chen [5], we wish to optimise the Yagi. Fundamentally, given a specific frequency, there are two characteristics to optimise: the element spacing and the element length. To optimise the directivity of such a Yagi antenna, it suffices to optimise both these quantities. Cheng and Chen are able to achieve this by considering *length* and *spatial 'perturbations'*. A given perturbation has an associated perturbation in the current through the elements and hence a perturbation in the radiation field generated by the antenna. Thus, by considering the associated change in the gain and hence directivity of the main lobe, we can isolate the optimum parameters of a Yagi-Uda antenna with N elements. The derivation of such is far too complex for this project, however in this section we will aim to experimentally deduce the theoretical values, by narrowing down the optimal parameters.

5.6.1 • Discussion of Directivity

The optimization of a Yagi-Uda antenna is a subtle process, indeed in this section section we analyse how even the slightest changes in the configuration a Yagi-Uda antenna alters its intensity profile and inevitably its directivity. To this end, let us first analyse a typical 3 element Yagi-Uda antenna, taking an arbitrary configuration, one might think optimal. We will attempt to optimise by brute force. Throughout, the distances we use, a, l, d, the vectors representing the radii, lengths and positions of the respective elements, are in **units of wavelength**.

Configuration 1:

$$l = [0.5, 0.5, 0.5]$$

$$d = [0, 0.25, 0.5]$$

$$a = [0.001, 0.001, 0.001]$$

We see that the radiation appears roughly uniform throughout space. In fact there is no general directivity, and we do not observe the greatest directivity at angles $\theta = \frac{\pi}{2}, \phi = 0$ as we would expect. We find a maximum directivity at $\theta = \frac{\pi}{2}, \phi = \frac{\pi}{2}$ given by:

$$D_{max} = 2.67$$

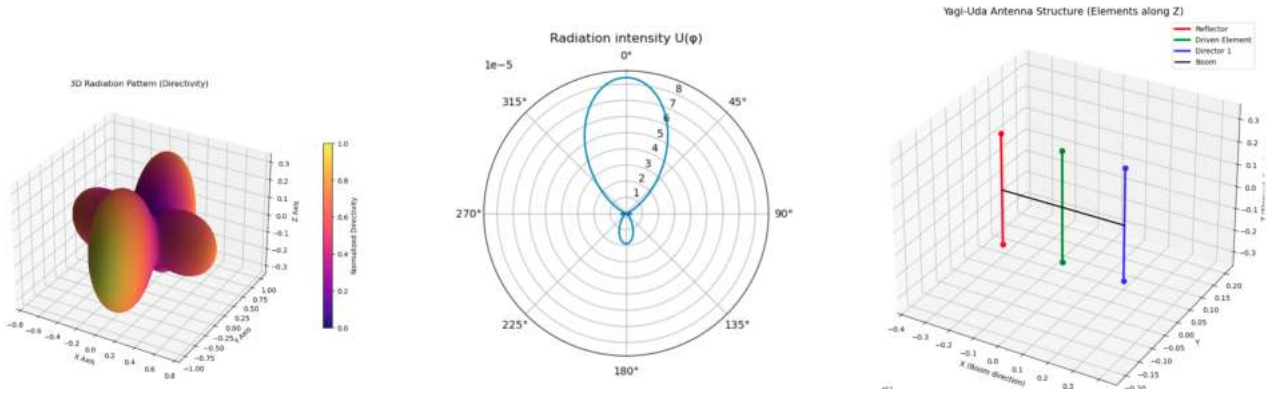

(a) 3D Plot (b) Azimuthal Plot (c) Spatial placement

Figure 22: Side-by-side comparison of radiation patterns for Yagi-Uda configuration 1

As we will see this is relatively poor. We should ensure the lengths of the elements are decreasing in order, to ensure that the radiation in directed towards the front-end (directors) of the Yagi-Uda antenna. In fact, this will worsen the mutual coupling between the elements, however it will generate a phase difference between the induced currents, in the elements, that optimises directivity. Hence, let us slightly increase (resp. decrease) the length of the reflector (resp. directors). Thus we will consider the following new vector for the lengths of the elements:

Configuration 2:

$$l' = [0.55, 0.50, 0.45]$$

Notice, this modification has significantly improved the directivity of our Yagi-Uda antenna. The intensity profile is no longer uniform, but directed towards $(\theta, \phi) = (\frac{\pi}{2}, 0)$ with a new maximum directivity of:

$$D_{max} = 5.65$$

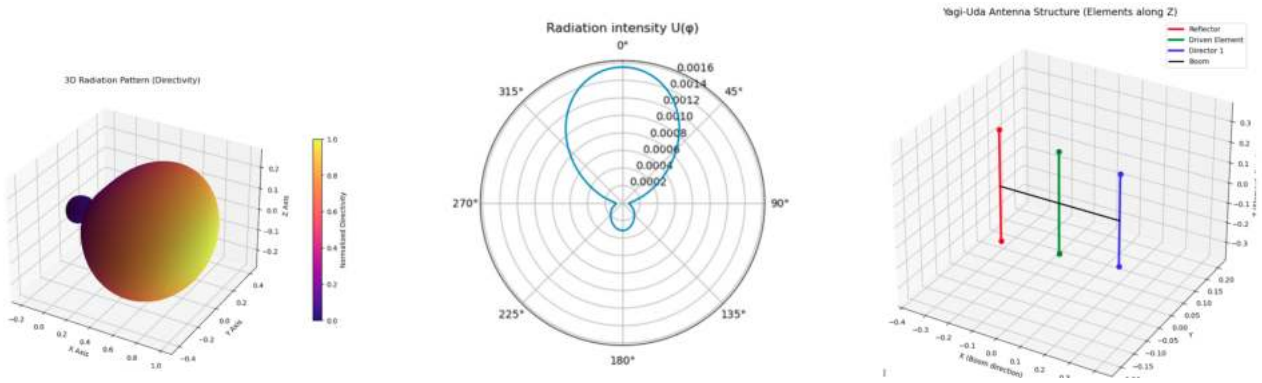

(a) 3D Plot (b) Azimuthal Plot (c) Spatial placement

Figure 23: Side-by-side comparison of radiation patterns for Yagi-Uda configuration 2

We have doubled our directivity simply by modifying the respective lengths of the elements by $5mm$. The reader may ask why we took this arbitrary value of $5mm$ as our respective difference in elements lengths and it is indeed entirely arbitrary. There is no indication this exact value yields the optimum directivity of the configuration. By the same logic, let us continue and consider a new lengths vector:

$$l' = [0.60, 0.50, 0.40]$$

Remarkably, we now find a lower maximum directivity, as by increasing the respective differences in length, the pattern has become more uniform. Indeed, the mutual coupling worsens. Furthermore, the phase between the currents in the driven elements, crucial to ensuring radiation interferes constructively at the front end of the antenna, are modified. In fact, it is these two parameters we in fact must optimise simultaneously; an optimum mutual coupling and respective phase differences in the elements, that optimises directivity. We find the pattern of the driven element now dominates more and ultimately a new D_{max} of:

$$D_{max} = 3.48$$

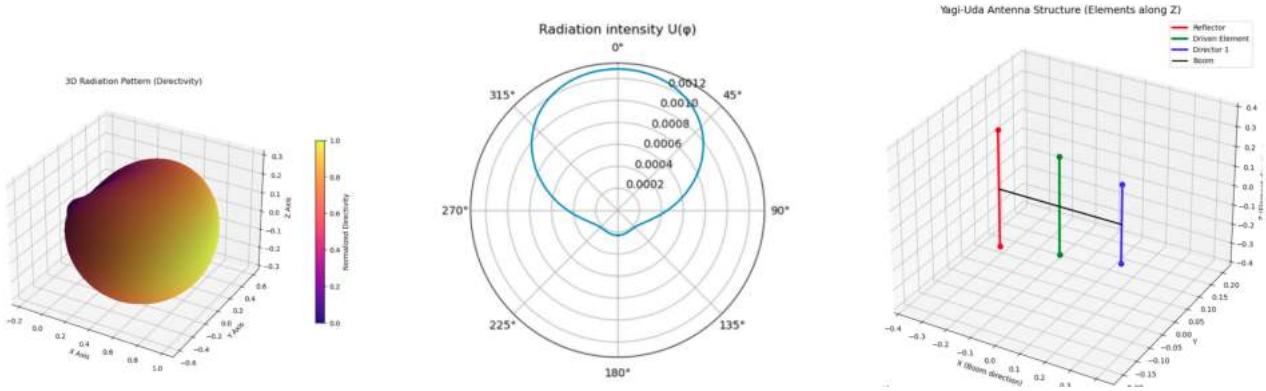

(a) 3D Plot (b) Azimuthal Plot (c) Spatial Placement

Figure 24: Side-by-side comparison of radiation patterns for Yagi-Uda configuration 3.

This suggests, fixing the position of the elements, an **optimum exists** in the length configuration, such an optimum will be derived experimentally in the next section.

An identical logic can be applied the position configuration of the Yagi-Uda antenna. Let us consider the following new position vector, fixing the length vector we found to be optimal l':

$$d' = [0, 0.3, 0.6]$$

We have the following radiation profile with an associated maximum directivity of $D_{max} = 4.35$:

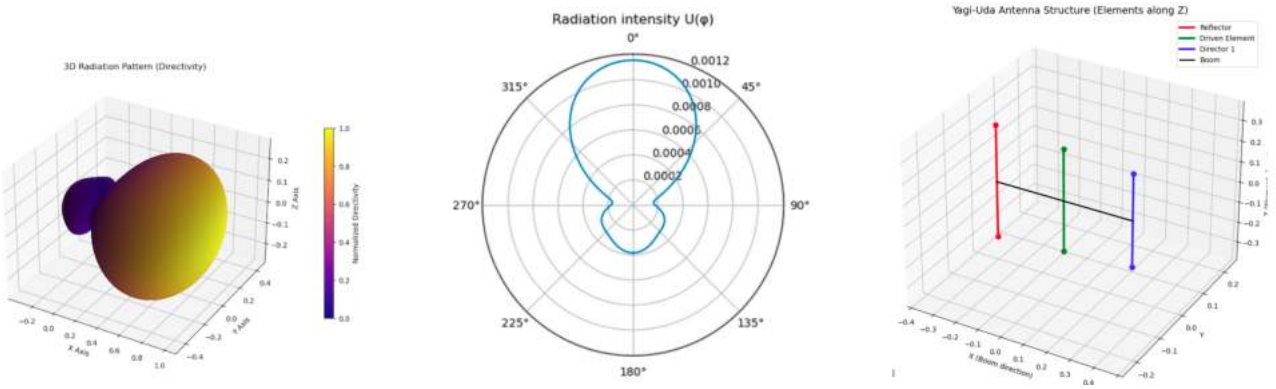

(a) 3D Polt (b) Azimuthal Plot (c) Spatial Placement

Figure 25: Side-by-side comparison of radiation patterns for Yagi-Uda configuration 4.

We have worsened our Yagi! Fundamentally, it follows an optimum exists in the position and lengths vector, that we will compute explicitly in the next section. Prior to such, as we commented throughout this section, it is the mutual coupling between elements and the respective phase differences between induced currents, that dictate the maximum directivity. Plots of such are provided in the remarks of the next section.

5.7 Optimisation

The optimisation of a Yagi-Uda antenna is complex. It is a non-linear, multivariable optimisation problem with some optimum configuration l_{op}, a_{op}, d_{op} satisfying:

$$l_{op}, d_{op}, a_{op} = \underset{l,d,a \in \mathbf{R^3}}{argmax} D_{max}(l, d, a)$$

We use a genetic algorithm, based on *natural selection*, which will preferentially select Yagi-Uda configurations with the greatest D_{max}. Initially, we associate to each Yagi-Uda configuration, modeled as an individual, its characteristics (l, d, a). Computing the associated D_{max}, the algorithm selects several of the optimum configurations to act as *parents* to the next generation. Through the use of a *blend crossover*, the attributes of the optimum Yagi-Uda antenna, the parents, are mixed to generate a new generation. Iterating this process over several generations, we indeed hope to find a plateau towards a maximum theoretical D_{max} with an associated optimum Yagi-Uda configuration.

Thus let us fix $a = [0.001, 0.001, 0.001]$, to maintain the thin wire approximation. Then, for a three element Yagi antenna configuration, we find the following with 100 generations, with population sizes of 100. The configuration below has an associated directivity of $D_{max} = 9.49$.

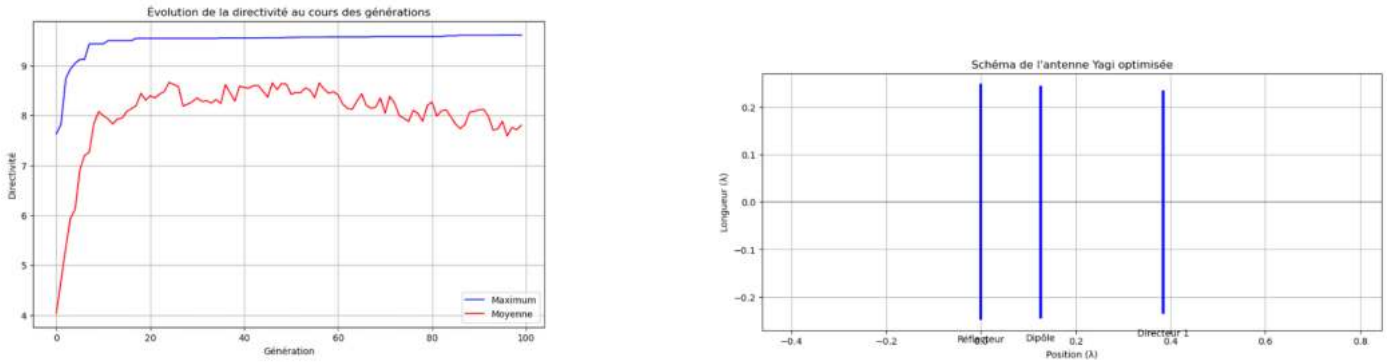

(a) Optimisation Process

(b) Optimal Configuration

Figure 26: Optimal Yagi-Uda Antenna

The physical parameters of this configuration are given by:

$$a = [0.001, 0.001, 0.001], l = [0.492, 0.485, 0.466], d = [0, 0.125, 0.384]$$

Below, the reader can find its associated intensity profile.

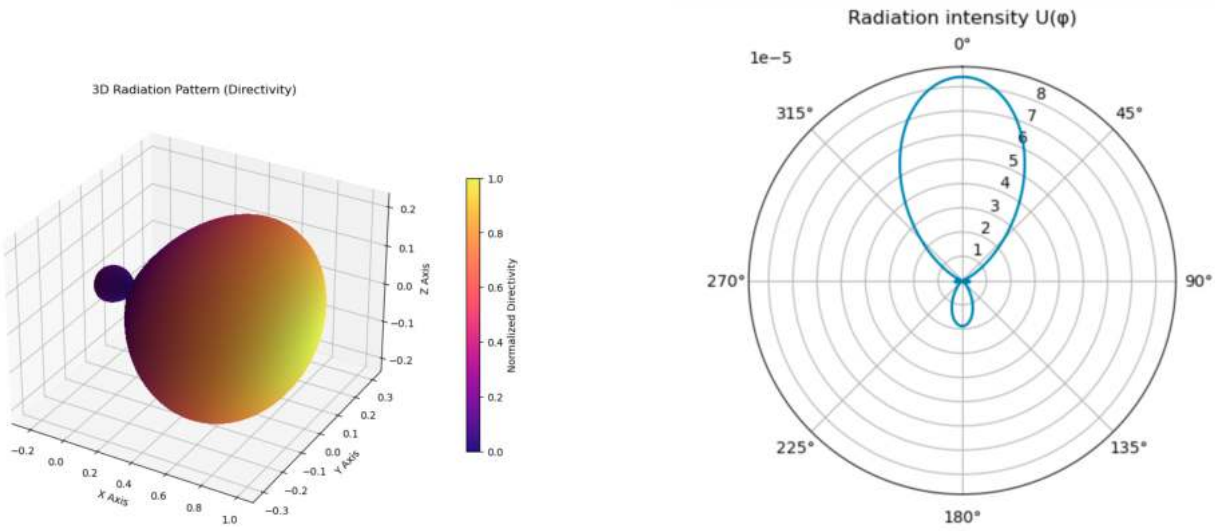

(a) 3D Plot

(b) Azimuthal Plot

Figure 27: Intensity Profile of Optimum Configuration

Remarks:

- This optimal configuration does seem rather similar to the Yagi-Uda antenna one finds in everyday life: the elements are decreasing in length and the driven element is closer to the reflector, than the director.
- We mentioned that this is a two fold process of optimising both the mutual coupling and the difference in phase of current between the elements, to yield the greatest directivity. Consider the director's and driven elements mutual coupling coefficient $Z_{2,3}$ as a function of difference in length. We have the following plots given below. Notice we have the strongest induced current when the difference in length is approximately -7%, this indicates that indeed a smaller length is expected.

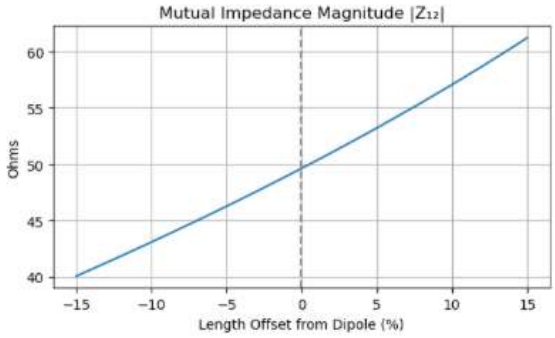

Figure 28: Mutual Impedance Magnitude

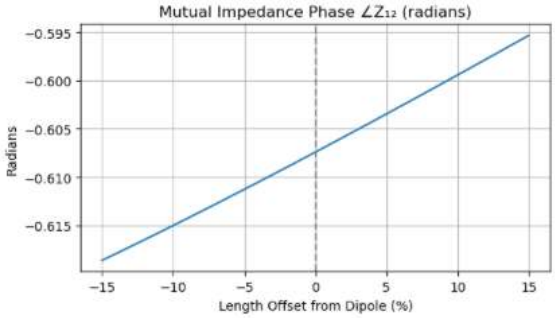

Figure 29: Mutual Impedance Phase

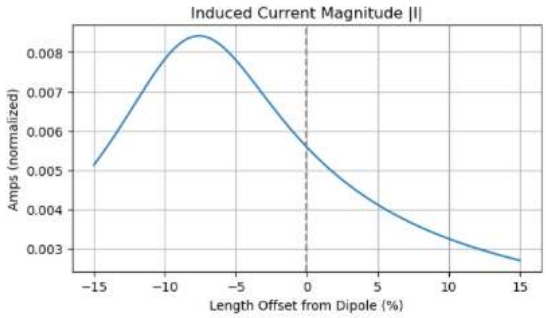

Figure 30: Induced Current Magnitude

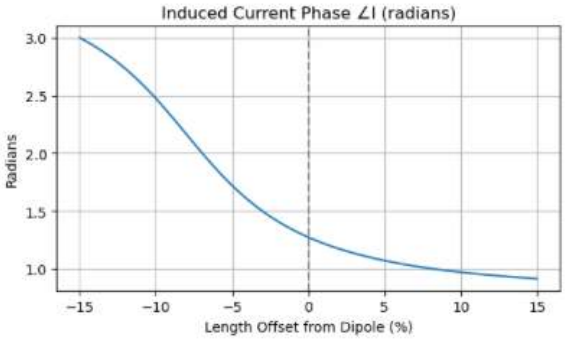

Figure 31: Induced Current Phase

Figure 32: Mutual coupling and induced current plots for Yagi-Uda antenna.

6 CONCLUSION AND POSSIBLE IMPROVEMENTS

This report has systematically investigated antenna directivity in multiple different configurations. From the mathematical approach of radiating fields to the complex antenna arrays, we explored the factors governing directional radiation. Although for simplicity, approximations such as the thin-wire and the general neglect of ground effects were made, the report puts in light the practical framework for understanding directivity. This study thus reinforces the theoretical understanding of antenna directivity. Future work could extend these analyses to more complex array geometries and relax some of our approximations which would result in more complex programming (e.g. Method of Moment).

7 CONTRIBUTIONS

Report: Armand + Mattheo + Max + Yanis

1. Intro + CCL: Armand
2. Radiating Fields : Max + Mattheo + Yanis

3. Antenna Parameters: Armand + Yanis
4. Linear Wire Antennas: Mattheo + Max
5. Uncoupled Antenna Arrays: Armand + Yanis
6. Coupled Antenna Arrays: Mattheo + Max
7. Appendix : Max + Mattheo + Armand
8. Bibliography: Mattheo + Max
9. MoM attempts: Mattheo + Max

Code + Simulations: **Mattheo** with Max and Yanis
Slides + Structure : Armand + Mattheo + Max

8 APPENDIX

8.1 Fundamental Physical Constants

We write below the well-known physical constants used throughout these notes.

- Speed of light in vacuum: $c = 299\,792\,458\,\mathrm{m\,s^{-1}}$
- Permittivity of vacuum: $\varepsilon_0 = 8.854\,187\,817 \times 10^{-12}\,\mathrm{F\,m^{-1}}$
- Permeability of vacuum: $\mu_0 = 4\pi \times 10^{-7}\,\mathrm{H/m}$
- Characteristic impedance of vacuum: $\eta = Z_0 = 376.730\,313\,461\,\Omega$
- Electron charge: $e = 1.602\,176\,462 \times 10^{-19}\,\mathrm{C}$
- Electron mass: $m_e = 9.109\,381\,887 \times 10^{-31}\,\mathrm{kg}$
- Planck constant: $h = 6.626\,068\,76 \times 10^{-34}\,\mathrm{J\,s}$

The characteristic impedance η (also denoted by Z_0) is derived from the relationship:

$$\eta = \sqrt{\frac{\mu_0}{\varepsilon_0}} = \mu_0 c$$

8.2 General Solution of the Inhomogeneous Wave Equation

The homogeneous and inhomogeneous wave equations are of the form

$$\left(c^2\Delta_n - \frac{\partial^2}{\partial t^2}\right)\psi = 0, \quad \left(c^2\Delta_n - \frac{\partial^2}{\partial t^2}\right)\psi = f,$$

where Δ_n is the n-dimensional Laplacian (and $n = 1, 2, 3$ are the most interesting dimensions for physics). We would like to find a Green function G, satisfying:

$$\left(c^2\Delta_3 - \frac{\partial^2}{\partial t^2}\right) G(t, \mathbf{x}) = -4\pi\delta(t)\delta(\mathbf{x}).$$

If we Fourier transform G in the t-direction:

$$G(t, \mathbf{x}) = \frac{1}{2\pi}\int_{\mathbb{R}} d\omega\, \tilde{G}(\omega, \mathbf{x}) e^{-i\omega t}$$

Then, it follows that the Fourier transform $\tilde{G}$ satisfies:

$$\left(c^2\Delta + \omega^2\right)\tilde{G}(\omega, \mathbf{x}) = -4\pi\delta(\mathbf{x})$$

We argue there are essentially two choices for the above:

$$\tilde{G}_{\pm}(\omega, \mathbf{x}) = \frac{e^{\pm i\omega|\mathbf{x}|}}{|\mathbf{x}|}.$$

Hence, reinserting this expression:

$$G_{\pm}(t,\mathbf{x}) = \frac{\delta(ct \mp |\mathbf{x}|)}{|\mathbf{x}|}.$$

The general solution to the inhomogeneous wave equation, using the so-called *retarded Green function* G_+, is then given by

$$\begin{aligned}\psi(t,\mathbf{x}) &= \psi_{\text{hom}}(t,\mathbf{x}) + \frac{1}{4\pi}\int_{\mathbb{R}^4} dt'\, d^3x'\, G_+(c(t-t'),\mathbf{x}-\mathbf{x}')f(t',\mathbf{x}') \\ &= \psi_{\text{hom}}(t,\mathbf{x}) + \frac{1}{4\pi}\int_{\mathbb{R}^4} dt'\, d^3x'\, \frac{\delta(c(t-t')-|\mathbf{x}-\mathbf{x}'|)}{|\mathbf{x}-\mathbf{x}'|}f(t',\mathbf{x}') \\ &= \psi_{\text{hom}}(t,\mathbf{x}) + \frac{1}{4\pi}\int_{\mathbb{R}^3} d^3x' \left(\frac{f(t',\mathbf{x}')}{|\mathbf{x}-\mathbf{x}'|}\right)_{ct'=ct-|\mathbf{x}-\mathbf{x}'|}\end{aligned}$$

Moreover, $\psi_{hom} = 0$ when we specify initial conditions for the source function $f(t,\mathbf{x})$. Thus, the practically important solution to the inhomogeneous wave equation reads:

$$\psi(t,\mathbf{x}) = \frac{1}{4\pi}\int_{\mathbb{R}^3} d^3x' \left(\frac{f(t',\mathbf{x}')}{|\mathbf{x}-\mathbf{x}'|}\right)_{ct'=ct-|\mathbf{x}-\mathbf{x}'|}$$

8.3 Ground effect

The notions and equations introduced in this section where extracted from [1]

The Ground effect refers to the significant influence that the Earth's surface has on the efficiency of Antennas. The effect of the ground is all the more important for antennas close to the ground. In practice the ground effects the parameters of the antennas such as radiation pattern impedance, efficiency and bandwidth. The frequencies of the antennas that are the most effected are Low Frequency and Medium Frequency Antennas.

As explained in [1], this is particularly evident in the input resistance. When the antenna's height is relatively small compared to the skin depth of the conducting earth, the input resistance's value is even greater than its theoretical value, leading to very low antenna efficiencies. An improvement to counter act these inefficiencies is to place radial wires or metallic disks on the ground.

There are multiple considerations that need to be taken into account to properly look into the effect of ground.

• Vertical Dipoles

Looking first at vertical dipoles and making observations in the far field, the direct and reflected components of the field are the following:

$$E_\theta^d = j\eta\frac{kI_0le^{-jkr_1}}{4\pi r_1}\sin\theta_1$$

$$E_\theta^r = jR_v\eta\frac{kI_0le^{-jkr_2}}{4\pi r_2}\sin\theta_2$$

Where the reflection coefficient R_v is given by:

$$R_v = \frac{\eta_0\cos\theta_i - \eta_1\cos\theta_t}{\eta_0\cos\theta_i + \eta_1\cos\theta_t} = -R_{\|}$$

With the following parameters:

$R_{\|}$ is the reflection coefficient for parallel polarization.

$$\eta_0 = \sqrt{\frac{\mu_0}{\epsilon_0}} = \text{intrinsic impedance of free-space (air)} \tag{41}$$

$$\eta_1 = \sqrt{\frac{j\omega\mu_1}{\sigma_1 + j\omega\epsilon_1}} = \text{intrinsic impedance of the ground} \tag{42}$$

θ_i = angle of incidence (relative to the normal)
θ_t = angle of refraction (relative to the normal)

The angles θ_i and θ_t are related by Snell's law of refraction

$$\gamma_0 \sin\theta_i = \gamma_1 \sin\theta_t \tag{43}$$

where

$\gamma_0 = jk_0$ = propagation constant for free-space (air)
k_0 = phase constant for free-space (air)
$\gamma_1 = (\alpha_1 + jk_1)$ = propagation constant for the ground
α_1 = attenuation constant for the ground
k_1 = phase constant for the ground

Using the far-field approximations:

$$r_1 \simeq r - hcos(\theta)$$
$$r_2 \simeq r + hcos(\theta)$$

, the total electric field above the ground ($z \geq 0$) can be written as

$$E_\theta = j\eta \frac{kI_0\ell e^{-jkr}}{4\pi r} \sin\theta \left[e^{jkh\cos\theta} + R_v e^{-jkh\cos\theta}\right] \quad z \geq 0 \tag{44}$$

where R_v is given above in this section of the appendix.

Using this solution we see that in the presence of the ground, the radiation toward the vertical direction ($60° > \theta > 0°$), is more intense than that of a perfect conductor, but for grazing angles ($\theta = 90°$) the radiation vanishes. The null field for $\theta = 90°$ is formed since R_v tends to -1 and θ tends to 90°. Thus the ground effects on the pattern of a vertically polarized antenna's are significantly different from those of a perfect conductor.

An example of the elevation plane amplitude patterns of an infinitesimal vertical dipole above a perfect electric dipole can be found below:

• Horizontal Dipoles

In a similar way to vertical dipoles we can retrieve the direct and reflected components with the reflection coefficient R_h given by:

$$R_h = \begin{cases} R_\perp & \text{for } \phi = 0°,\ 180° \text{ plane} \\ R_\parallel & \text{for } \phi = 90°,\ 270° \text{ plane} \end{cases}$$

Where $R_\parallel$ is the reflection coefficient for parallel polarization and $R_\perp$ is given by:

$$R_\perp = \frac{\eta_1 \cos\theta_i - \eta_0 \cos\theta_t}{\eta_1 \cos\theta_i + \eta_0 \cos\theta_t}$$

The angles θ_i and θ_t are again related by Snell's law as stated in the vertical dipole sub section.
using the far field approximations:

$$\begin{aligned} r_1 &\simeq r - h\cos\theta && \text{for phase variations} \\ r_2 &\simeq r + h\cos\theta && \text{for phase variations} \\ r_1 &\simeq r_2 \simeq r && \text{for amplitude variations} \end{aligned}$$

The total field above ground ($z \geq h$) is:

$$E_\psi = j\eta \frac{kI_0\ell e^{-jkr}}{4\pi r}\sqrt{1-\sin^2\theta\sin^2\phi}\left[e^{jkh\cos\theta} + R_h e^{-jkh\cos\theta}\right], \quad z \geq h$$

With R_h as defined above.

We examine R_h and notice that for a ground medium the values of R_h for most observation angles are around -1 (the necessary value of R_h for a perfect conductor). For grazing angles, θ_i tends to 90°, the values of R_h approach -1 rapidly. Hence we can deduce that the relative pattern of the ground is not that different from that of a perfect conductor, a difference to the vertical dipole.

- Why we can neglect the ground effect in our cases

Although the ground effect always has some influence on the performance of antennas, we can neglect the ground effect. We have placed ourselves in the far field, hence we have large observation angles. As noted in [7] we can assume that the earth is flat for observation angles of about $57.3/(ka)^{1/3}$ degrees from grazing, which is generally greater than about about 3°. In these regions the influence of the ground on the antenna's radiation pattern is minimal and thus we either have a perfect conductor (horizontal dipole) or free space (vertical dipole).

Alternative assumptions that can justify the neglect of the ground effect is short wavelengths relative to the earth's curvature, this is generally the case for very high frequency antennas.

8.4 Gauge transformation

Despite being useful tools, what matters is not the potentials but the resulting fields. We will show that the electromagnetic fields will not change under the following *gauge transformations*:

$$V \to V' = V - \frac{\partial f}{\partial t} \quad \boldsymbol{A} \to \boldsymbol{A}' = \boldsymbol{A} + \boldsymbol{\nabla} f$$

for any scalar function $f(\boldsymbol{r}, t)$.

Observe first that for any scalar function $f : (x, y, z, t) \to f(x, y, z, t)$

$$\nabla \times \nabla f = \begin{bmatrix} \partial_x \\ \partial_y \\ \partial_z \end{bmatrix} \times \begin{bmatrix} \partial_x f \\ \partial_y f \\ \partial_z f \end{bmatrix} = \begin{bmatrix} \partial_y\partial_z f - \partial_z\partial_y f \\ \partial_z\partial_x f - \partial_x\partial_z f \\ \partial_x\partial_y f - \partial_y\partial_x f \end{bmatrix} = \vec{0}$$

according to Schwarz theorem stating that $\partial_y\partial_x f = \partial_x\partial_y f$ if f is C^1 which will be assumed here.

Therefore, for vector potential $\boldsymbol{A}' = \boldsymbol{A} + \boldsymbol{\nabla} f$, the new magnetic field reads:

$$\boldsymbol{B}' = \boldsymbol{\nabla} \times (\boldsymbol{A} + \boldsymbol{\nabla} f) = \boldsymbol{\nabla} \times \boldsymbol{A} + \boldsymbol{\nabla} \times \boldsymbol{\nabla} f = \boldsymbol{B}$$

meaning that $\boldsymbol{B}$ is left invariant with this transformation on the potential.

We proceed in the same way for the electric field:

$$\boldsymbol{E}' = -\boldsymbol{\nabla} V' - \partial_t \boldsymbol{A}' = -\boldsymbol{\nabla}(V - \partial_t f) - \partial_t(\boldsymbol{A} + \boldsymbol{\nabla} f) = -\boldsymbol{\nabla} V - \partial_t \boldsymbol{A} = \boldsymbol{E}$$

since $\partial_t \partial_i f = \partial_i \partial_t f$ for any $i = x, y, z$. This shows that the gauge transformation leaves $\boldsymbol{E}$ invariant.

We have used cartesian coordinates, but it would have worked with any other system.

This freedom in selecting the potentials allows us to impose some convenient constraints between them as long as they respect the previous transformations. In particular, in discussing radiation problems, we will impose the Lorenz condition.

8.5 Numerical integration

When we are not able to compute an integral over a closed surface (or over a finite length) by hand (notably in the case of power), we can still divide the interval of integration into smaller ones, and sum over a fixed value within each interval, provided that the integrand is smooth enough (in the sense that it does not have high and sharp peaks). Note that this criterion is inherently dependent on the chosen value of N. A larger N allows for the handling of more rapidly varying functions. To be more explicit, suppose we have a function $f : \theta \to f(\theta)$, we want to integrate over the compact interval $[0, \pi]$ (see Standing waves antenna), then, choosing an integer N large enough,

$$\int_0^\pi f(\theta) d\theta \approx \sum_{i=1}^{N} f(\theta_i) \delta\theta_i$$

with $\theta_i = (i - \frac{1}{2})\frac{\pi}{N} \in [(i-1)\frac{\pi}{N}, i\frac{\pi}{N}]$ the midpoint in each sub-interval and $\delta\theta_i = \frac{\pi}{N}$ the size of each interval. We can observe that $\bigcup_{i=1}^{N} [(i-1)\frac{\pi}{N}, i\frac{\pi}{N}] = [0, \pi]$. This method can be quickly implemented to compute the power radiated, knowing that increasing N reduces the margin of error.
The reader can find our Matlab code used for the half-wave antenna radiated power by clicking here.

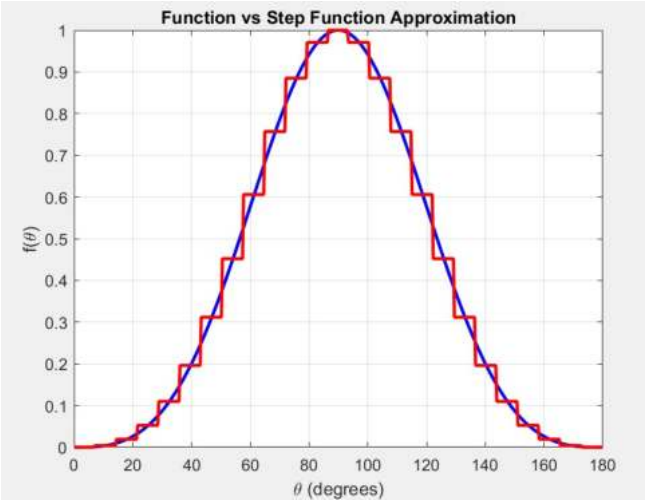

Figure 33: Illustration of the approximation for N = 200

8.6 Mathematics toolbox

- Vectorial identities

Cylindrical coordinates

- Gradient:
$$\nabla f = \frac{\partial f}{\partial r}\hat{\mathbf{e}}_r + \frac{1}{r}\frac{\partial f}{\partial \phi}\hat{\mathbf{e}}_\phi + \frac{\partial f}{\partial z}\hat{\mathbf{e}}_z$$
- Divergence:
$$\nabla \cdot \mathbf{A} = \frac{1}{r}\frac{\partial}{\partial r}(rA_r) + \frac{1}{r}\frac{\partial A_\phi}{\partial \phi} + \frac{\partial A_z}{\partial z}$$
- Curl:
$$\nabla \times \mathbf{A} = \left(\frac{1}{r}\frac{\partial A_z}{\partial \phi} - \frac{\partial A_\phi}{\partial z}\right)\hat{\mathbf{e}}_r + \left(\frac{\partial A_r}{\partial z} - \frac{\partial A_z}{\partial r}\right)\hat{\mathbf{e}}_\phi + \frac{1}{r}\left(\frac{\partial}{\partial r}(rA_\phi) - \frac{\partial A_r}{\partial \phi}\right)\hat{\mathbf{e}}_z$$
- Laplacian:
$$\nabla^2 f = \frac{1}{\rho}\frac{\partial}{\partial \rho}\left(\rho\frac{\partial f}{\partial \rho}\right) + \frac{1}{\rho^2}\frac{\partial^2 f}{\partial \phi^2} + \frac{\partial^2 f}{\partial z^2}$$

Spherical coordinates

- Gradient:
$$\nabla f = \frac{\partial f}{\partial r}\hat{\mathbf{e}}_r + \frac{1}{r}\frac{\partial f}{\partial \theta}\hat{\mathbf{e}}_\theta + \frac{1}{r\sin\theta}\frac{\partial f}{\partial \phi}\hat{\mathbf{e}}_\phi$$
- Divergence:
$$\nabla \cdot \mathbf{A} = \frac{1}{r^2}\frac{\partial}{\partial r}(r^2 A_r) + \frac{1}{r\sin\theta}\frac{\partial}{\partial \theta}(\sin\theta A_\theta) + \frac{1}{r\sin\theta}\frac{\partial A_\phi}{\partial \phi}$$
- Curl:
$$\nabla \times \mathbf{A} = \frac{1}{r\sin\theta}\left[\frac{\partial}{\partial \theta}(\sin\theta A_\phi) - \frac{\partial A_\theta}{\partial \phi}\right]\hat{\mathbf{e}}_r + \frac{1}{r}\left[\frac{1}{\sin\theta}\frac{\partial A_r}{\partial \phi} - \frac{\partial}{\partial r}(rA_\phi)\right]\hat{\mathbf{e}}_\theta + \frac{1}{r}\left[\frac{\partial}{\partial r}(rA_\theta) - \frac{\partial A_r}{\partial \theta}\right]\hat{\mathbf{e}}_\phi$$
- Laplacian:
$$\nabla^2 f = \frac{1}{r^2}\frac{\partial}{\partial r}\left(r^2\frac{\partial f}{\partial r}\right) + \frac{1}{r^2\sin\theta}\frac{\partial}{\partial \theta}\left(\sin\theta\frac{\partial f}{\partial \theta}\right) + \frac{1}{r^2\sin^2\theta}\frac{\partial^2 f}{\partial \phi^2}$$

- Differential Identities

$$\nabla \times (\nabla \times \mathbf{A}) = \nabla(\nabla \cdot \mathbf{A}) - \nabla^2 \mathbf{A}$$
$$\nabla \cdot (\alpha \boldsymbol{A}) = \alpha \nabla \cdot \boldsymbol{A} + \nabla\alpha \cdot \boldsymbol{A}$$

8.7 Detail of calculations made throughout the report.

- Proof of the identity from the section Standing Wave Antennas

$$\begin{aligned}\int e^{ax}\sin(bx+c)dx &= \frac{1}{2i}\int e^{(a+ib)x+ic} - e^{-(ib-a)x-ic}dx \\ &= \frac{e^{ic}}{2i}\left[\frac{e^{(a+ib)x}}{(a+ib)x}\right] - \frac{e^{-ic}}{2i}\left[\frac{e^{-(ib-a)x}}{(a-ib)x}\right] \\ &= \frac{e^{ic}}{2i(a^2+b^2}\left[(a-ib)e^{(a+ib)x}\right] - \frac{e^{-ic}}{2i(a^2+b^2}\left[(a+ib)e^{-(ib-a)x}\right] \\ &= \frac{e^{ax}}{a^2+b^2}\left[\frac{-ib(e^{-i(bx+c)}+e^{i(bx+c)})}{2i} + \frac{a(e^{i(bx+c)}-e^{-i(bx+c)})}{2i}\right] \\ &= \frac{e^{ax}}{a^2+b^2}[a\sin(bx+c) - b\cos(bx+c)]\end{aligned}$$

- Further details of the calculations for F_θ

$$F_\theta = \sin\theta\int_{-l/2}^{l/2} I_0\sin\left(k(\frac{l}{2}-|z|)\right)e^{ik\cdot z'\cos(\theta)}dz'$$
$$F_\phi = 0$$

We are left to integrating this integral. First, we write it as:

$$F_\theta = I_0\sin\theta\left(\int_{-l/2}^{0}\sin\left(k(\frac{l}{2}+z')\right)e^{ik\cdot z'\cos(\theta)}dz' + \int_0^{l/2}\sin\left(k(\frac{l}{2}-z')\right)e^{ik\cdot z'\cos(\theta)}dz'\right)$$

Taking $a = ik\cos\theta$, $b = \pm k$ and $c = \frac{kl}{2}$, we recognize eq.24. Therefore, we get for the first integral:

$$\begin{aligned}\int_{-l/2}^{0}\sin\left(k(\frac{l}{2}+z')\right)e^{ik\cdot z'\cos(\theta)}dz' &= \left[\frac{e^{ik\cos\theta z'}}{-k^2\cos^2\theta+k^2}[ik\cos\theta\sin\left(kz'+\frac{kl}{2}\right) - k\cos\left(kz'+\frac{kl}{2}\right)\right]_{-l/2}^{0} \\ &= \frac{1}{k\sin^2\theta}\left[i\cos\theta\sin\left(\frac{kl}{2}\right) - \cos\left(\frac{kl}{2}\right) - e^{-ik\cos\theta l/2}\right]\end{aligned}$$

Similarly, for the second integral

$$\begin{aligned}\int_0^{l/2}\sin\left(k(\frac{l}{2}-z')\right)e^{ik\cdot z'\cos(\theta)}dz' &= \left[\frac{e^{ik\cos\theta z'}}{-k^2\cos^2\theta+k^2}[ik\cos\theta\sin\left(-kz'+\frac{kl}{2}\right) + k\cos\left(-kz'+\frac{kl}{2}\right)\right]_{0}^{l/2} \\ &= \frac{1}{k\sin^2\theta}\left[e^{ik\cos\theta l/2} - i\cos\theta\sin\left(\frac{kl}{2}\right) - \cos\left(\frac{kl}{2}\right)\right]\end{aligned}$$

Adding the two yields:

$$\begin{aligned}F_\theta &= I_0\sin\theta\ \frac{1}{k\sin^2\theta}\left[e^{ik\cos\theta l/2} + e^{-ik\cos\theta l/2} - 2\cos\left(\frac{kl}{2}\right)\right] \\ &= 2I_0\frac{1}{k\sin\theta}\left[\cos(k\cos\theta l/2) - \cos\left(\frac{kl}{2}\right)\right]\end{aligned}$$

• Verification of the validity of the dispersion relation

One can verify that the dispersion relation $\omega = kc$ is indeed verified in the far-field, i.e. neglecting high-order spatial terms going like $O(1/r^2)$ and higher. For instance,

$$\partial_r(\frac{e^{-ikr}}{r}) = \frac{-ikre^{-ikr} - e^{-ikr}}{r^2}$$

$$\partial_r(r^2\partial_r\left(\frac{e^{-ikr}}{r}\right)) = \partial_r(-ikre^{-ikr} - e^{-ikr}) = \cancel{-ike^{-ikr}} - k^2re^{-ikr} + \cancel{ike^{-ikr}}$$

implying that $\frac{1}{r^2}\partial_r(r^2\partial_r\boldsymbol{E}) = -k^2\boldsymbol{E}$

$$\partial_\phi\boldsymbol{E} = \boldsymbol{0}$$

$$\frac{1}{r^2\sin\theta}\partial_\theta(\sin\theta\partial_\theta\boldsymbol{E}) \sim O(\frac{1}{r^3})$$

$$\partial_t^2\boldsymbol{E} = -\omega^2\boldsymbol{E}$$

Using the expression of the Laplacian in spherical coordinates, We plug these results into the wave equation ($\rho = 0$, $\boldsymbol{j} = \boldsymbol{0}$) to get $k^2 \approx \omega^2/c^2$ for r large.

• Detailed calculation of Z_{pq}

$$Z_{pq} = \frac{j\eta}{4\pi k}\int_{-h_p}^{h_p}\int_{-h_q}^{h_q}\frac{I_p(z)I_q(z')}{I_pI_q}(\partial_z^2 + k^2)G_{pq}(z-z')\,dz'\,dz$$

We will deal with almost half-wave antenna. If we assume that the currents are sinusoidal, that is, for $p = 1, 2$:

Denoting for the moment $I(z) = \sin(k(h_p - |z|))$, we will focus on the term in parenthesis:

$$\int_{-h_p}^{h_p} I(z)(\partial_z^2 + k^2)G_{pq}(z-z')dz = k^2\int_{-h_p}^{h_p} I(z)G_{pq}(z-z')dz + \int_{-h_p}^{h_p} I(z)\partial_z^2G_{pq}(z-z')dz = (1) + (2)$$

Remark that $I(h_p) = I(-h_p) = 0$. Integrating by parts the second term yields:

$$\begin{aligned}(2) &= \cancel{[I(z)\partial_zG_{pq}(z-z')]_{-h_p}^{h_p}} - \int_{-h_p}^{h_p} I'(z)\partial_zG_{pq}(z-z')dz \\ &= -\left[I'(z)G_{pq}(z-z')\right]_{-h_p}^{h_p} + \int_{-h_p}^{h_p} I''(z)G_{pq}(z-z')dz\end{aligned}$$

In addition, we have:

$$I(z) = \begin{cases}\sin(k(h_p - z)) & \text{if } 0 \geq z \geq h_p \\ \sin(k(h_p + z)) & \text{if } 0 \leq z \leq -h_p\end{cases}$$

$$\implies I'(z) = \begin{cases}-k\cos(k(h_p - z)) & \text{if } 0 \geq z \geq h_p \\ k\cos(k(h_p + z)) & \text{if } 0 \leq z \leq -h_p\end{cases}$$

$$\implies I''(z) = \begin{cases}-k^2\sin(k(h_p - z)) & \text{if } 0 \geq z \geq h_p \\ -k^2\sin(k(h_p + z)) & \text{if } 0 \leq z \leq -h_p\end{cases} = -k^2\sin(k(h_p - |z|)) = -k^2I(z)$$

This gives:

$$\begin{aligned}(1)+(2) &= k^2\int_{-h_p}^{h_p} I(z)G_{pq}(z-z')dz - \left[I'(z)G_{pq}(z-z')\right]_{-h_p}^{h_p} + \int_{-h_p}^{h_p} I''(z)G_{pq}(z-z')dz \\ &= \cancel{k^2\int_{-h_p}^{h_p} I(z)G_{pq}(z-z')dz} - \cancel{k^2\int_{-h_p}^{h_p} I(z)G_{pq}(z-z')dz} - \left[I'(z)G_{pq}(z-z')\right]_{-h_p}^{h_p}\end{aligned}$$

We are left with:

$$\begin{aligned}-\left[I'(z)G_{pq}(z-z')\right]_{-h_p}^{h_p} &= -\left[I'(z)G_{pq}(z-z')\right]_{-h_p}^{0} - \left[I'(z)G_{pq}(z-z')\right]_{0}^{h_p} \\ &= -k\cos(kh_p)G_{pq}(-z') + k\cos(k(h_p-h_p))G_{pq}(-h_p-z') \\ &+ k\cos(k(h_p-h_p))G_{pq}(h_p-z') - k\cos(kh_p)G_{pq}(-z') \\ &= kG_{pq}(-h_p-z') + kG_{pq}(h_p-z') - 2k\cos(kh_p)G_{pq}(-z')\end{aligned}$$

$$I_p(z) = I_p\frac{\sin(k(h_p-|z|))}{\sin(kh_p)} \tag{45}$$

with I_p to be determined. Then, in the expression of Z_{pq} the ratios $I_p(z)/I_p$ and hence Z_{pq} become independent of the input currents at the antenna terminals and depend only on the geometry of the antennas:

Notice that we have split the interval in two between $I'(z)$ has a discontinuity at $z=0$.

$$Z_{pq} = \frac{j\eta}{4\pi k}\int_{-h_p}^{h_p}\int_{-h_q}^{h_q}\frac{\sin(k(h_p-|z|))}{\sin(kh_p)}\frac{\sin(k(h_q-|z'|))}{\sin(kh_q)}(\partial_z^2+k^2)G_{pq}(z-z')\,dz'\,dz \tag{46}$$

8.8 Python Codes

Please find here the link to our GitHub repository, where all codes illustrating these notes are stored

REFERENCES

[1] Balanis, C. A. (2016). *Antenna theory: Analysis and design* (4th ed.). Wiley.

[2] Volakis, J. L. (Ed.). (2007). *Antenna engineering handbook* (4th ed.). McGraw-Hill.

[3] Zangwill, A. (2018) *Modern electrodynamics*. Cambridge: Cambridge University Press.

[4] Couairon, A. & Cadiz, F. (2025) *Classical Electrodynamics* Ecole Polytechnique

[5] D. Cheng and C. Chen, (1972) *Optimum element spacings for Yagi-Uda arrays,* Antennas and Propagation Society International Symposium, Williamsburg, VA, USA, 1972, pp. 119-120.

[6] Q.J, (1997) *Using genetic algorithms to optimise model parameters*, Environmental Modelling & Software, 12(1), pp. 27–34.